Response to Referee #1

Abstract Line 30 change since to during

L49 define WMO

Modified

L81 and throughout: Figure numbers missing

Modified

L125 I find this hard to believe, an RS41 is about 200 USD in Europe. Maybe omit this sentence about the Vaisala price comparison and place a sole focus on the low cost of the device

Modified, however, as a side note, we are paying around 300 USD here in Taiwan.

L251: Define θ¬e,

Modified

L252: A short line is needed here summarising the boundary layer height retrieval method from the paper mentioned. The PBL shown in figure 12 does not look correct especially for days 3 and 4

Thank you for your comments, we modified the section 4 to include the summary of boundary layer height retrieval method.

The reason might be that day 3 we face some restrictions limit our flight plan so that it lacks the critical daytime data, and as for day 4, the figure only contains up to 6 am, so it might seem weird.

Section 4: Include a small description of the synoptic meteorology that was happening during those days, why were the latter two days warmer etc.

You need to plot meteorological data from the ascents into the typhoon to show the uses of the novel system.

Thank you for your comments, we added Figure 17 for the sensor data, and Figure 15 for showing the synoptic chart.

Figure 11 make these box plots so the distribution of the time lags and use a suitable y scale

Modified, though we think that it might be better to remove the bar plot since we already have the statistics in Table 4, so we remove the bottom plot and added numbers to the description.

Figure 12: Is this height above sea level or above the ground

It is above sea level.

Response to Referee #2

The authors have responded to all of my comments reasonably in the reply letter. However, I am surprised that the authors have not included the first two figures shown in the reply letter, i.e., “2018/07/15 18h LST” and “temporal changes of vertical profiles”. I believe including these two figures in the revised manuscript would be necessary for full understanding of the performance and would have result in more positive impression to the instrument.

Thank you for your comments, we added both plot in our manuscript in section 3 Figure 10 and Figure 11.

Draftable Comparison Export

This document is an exported comparison with limited functionality, generated by Draftable Desktop. To access full functionality, use Draftable's powerful comparison viewer in any of our products.

Left document:	StormTracker_manuscript_v5 (3).pdf
Right document:	StormTracker_manuscript_v6.1.pdf

What is this document?

This is a comparison of two documents. The two documents are interleaved such that the left document is displayed on odd pages and the right document is displayed on even pages.

Is there a specific way I should view this file?

This document is intended to be viewed in Two Page Continuous mode (or sometimes called 'Two Page Scrolling'). It should open in this mode by default when using Adobe Acrobat and most popular PDF readers.

If the document opens in a different view, you can often change this in the settings. In Adobe Acrobat, go to **View > Page Display > Two Page Scrolling**.

Why are there blank pages?

Blank pages are inserted to keep both documents as aligned as much as possible.

How do I read the changes?

Text deleted from the left document and, hence, not in right document is highlighted red. Text added to the right document and, hence, not in left document is highlighted green.

Tip for printing

When printing this document, we recommend printing double-sided and include this first page. This will result in the matching text being displayed on different pages and easily readable, much like a book.

For more information

Draftable offers powerful document comparison solutions for all use-cases. To view our products, please visit our website: draftable.com.

The Development of the "Storm Tracker" and its Applications for Atmospheric High-resolution Upper-air Observations

Wei-Chun Hwang[1] Po-Hsiung Lin[1] and Hungjui Yu[1]

[1] Department of Atmospheric Sciences, National Taiwan University, No. 1, Sec. 4, Roosevelt Road, Taipei, Taiwan, 106.

Correspondence to Po-Hsiung Lin (polin@ntu.edu.tw)

https://scholars.lib.ntu.edu.tw/cris/rp/rp07764

The Development of the "Storm Tracker" and its Applications for Atmospheric High-resolution Upper-air Observations

Wei-Chun Hwang[1] Po-Hsiung Lin[1] and Hungjui Yu[1]

[1] Department of Atmospheric Sciences, National Taiwan University, No. 1, Sec. 4, Roosevelt Road, Taipei, Taiwan, 106.

Correspondence to Po-Hsiung Lin (polin@ntu.edu.tw)

https://scholars.lib.ntu.edu.tw/cris/rp/rp07764

Abstract

In this study, we introduce a newly-developed upper-air observational instrument for atmospheric research. The "Storm Tracker" (or "NTU mini-Radiosonde"), is an ultra-lightweight (about 20g including battery), multi-channel simultaneous capable radiosonde designed by the Department of Atmospheric Sciences at National Taiwan University. Developed since 2016, the Storm Tracker aims to provide an alternative for observation of atmospheric vertical profiles with a high temporal resolution, especially lower-level atmosphere under severe weather such as extreme thunderstorms and tropical cyclones.

Field experiments were conducted as trial runs at Wu-Chi, Taichung, Taiwan, to examine the ability of the Storm Tracker on boundary layer observation, in addition to the intercomparison between the Storm Tracker and the widely used Vaisala RS41-SGP radiosonde. Among the co-launches of the Storm Tracker and Vaisala RS41 radiosondes, the measurements of pressure, wind speed, and wind direction are highly consistent between the Storm Tracker and Vaisala RS41-SGP. However, a significant daytime warm bias was found due to solar heating. A metal shield specifically for the Storm Tracker was thus installed and showed mitigation for the warm biases and the overall variance.

With the much lower costs of the radiosondes and the simultaneous multi-channel receiver, the Storm Tracker system has shown great potential for high-frequency observational needs in atmospheric research.

Abstract

In this study, we introduce a newly-developed upper-air observational instrument for atmospheric research. The "Storm Tracker" (or "NTU mini-Radiosonde"), is an ultra-lightweight (about 20g including battery), multi-channel simultaneous capable radiosonde designed by the Department of Atmospheric Sciences at National Taiwan University. Developed during 2016, the Storm Tracker aims to provide an alternative for observation of atmospheric vertical profiles with a high temporal resolution, especially lower-level atmosphere under severe weather such as extreme thunderstorms and tropical cyclones.

Field experiments were conducted as trial runs at Wu-Chi, Taichung, Taiwan, to examine the ability of the Storm Tracker on boundary layer observation, in addition to the intercomparison between the Storm Tracker and the widely used Vaisala RS41-SGP radiosonde. Among the co-launches of the Storm Tracker and Vaisala RS41 radiosondes, the measurements of pressure, wind speed, and wind direction are highly consistent between the measurements of the Storm Tracker and the Vaisala RS41-SGP. However, a significant daytime warm bias in the Storm Tracker was found due to solar heating. A metal shield specifically for the Storm Tracker was thus installed and showed mitigation for the warm biases and the overall variance.

With the much lower costs of the radiosondes and the simultaneous multi-channel receiver, the Storm Tracker system has shown great potential for high-frequency observational needs in atmospheric research.

1. Introduction

With a long history of development, the upper-air radiosonde has been one of the essential and the most reliable method to measure the atmosphere above us so far. Operational weather agencies worldwide share their daily to twice-a-day (00UTC and 12UTC) radiosonde observational data through WMO GTS (Global Telecommunication System) for synoptic weather analysis and numerical model forecast. According to the European Centre for Medium-Range Weather Forecasts (ECMWF), in 2017, there are about 818 upper-air radiosonde stations worldwide in addition to more than twelve radiosonde manufactures (Ingleby 2017). So far, most radiosonde manufacturers had participated in the field inter-comparison program hosted by World Meteorological Organization (WMO) throughout 1984–2010, and there were 11 different types of operational radiosondes processed in the recent inter-comparison experiment at Yangjiang, China in 2011 (Nash et al. 2011)

Among all different types of radiosondes, the mostly used Vaisala RS41 radiosonde weighs 110g, and the previous version RS92 weighs 280g. The Japan radiosonde from Meisei Corporation, iMS-100 weighs 38g only, which is so far the lightest operational radiosonde. However, occasionally there are needs for many radiosondes within a short period of time to acquire higher temporal resolution data. For the atmospheric research community, most of these radiosondes on the market are often a burden regarding the research budget when a large amount is needed. Secondly, the lighter the radiosonde weighs, the smaller the balloons and the less the helium is needed. Lighter radiosondes also enable launching using a low-cost constant plastic balloon, which can also be deployed as a drift-sonde. In section 4, we will present two scenarios, one is vertical profiling, and the other is drift-sonde operation.

In this study, we introduce a newly-developed, smaller, lighter, and cheaper upper-air radiosonde system designed with the capability of simultaneously receiving multiple radiosondes, which is explicitly for high temporal resolution observations on mesoscale

1. Introduction

With a long history of development, the upper-air radiosonde has been one of the essential and the most reliable method to measure the atmosphere above us so far. Operational weather agencies worldwide share their daily to twice-a-day (00UTC and 12UTC) radiosonde observational data through WMO (World Meteorological Organization) GTS (Global Telecommunication System) for synoptic weather analysis and numerical model forecast. According to the European Centre for Medium-Range Weather Forecasts (ECMWF), in 2017, there are about 818 upper-air radiosonde stations worldwide in addition to more than twelve radiosonde manufactures (Ingleby 2017). So far, most radiosonde manufacturers had participated in the field inter-comparison program hosted by World Meteorological Organization (WMO) throughout 1984–2010, and there were 11 different types of operational radiosondes processed in the recent inter-comparison experiment at Yangjiang, China in 2011 (Nash et al. 2011)

Among all different types of radiosondes, the mostly used Vaisala RS41 radiosonde weighs 110g, and the previous version RS92 weighs 280g. The Japan radiosonde from Meisei Corporation, iMS-100 weighs 38g only, which is so far the lightest operational radiosonde. However, occasionally there are needs for many radiosondes within a short period of time to acquire higher temporal resolution data. For the atmospheric research community, most of these radiosondes on the market are often a burden regarding the research budget when many radiosondes are needed. Secondly, the lighter the radiosonde weighs, the smaller the balloons and the less the helium is needed. Lighter radiosondes also enable launches using a low-cost constant plastic balloon, which can also be deployed as a drift-sonde. In section 4, we will present two scenarios, one is vertical profiling, and the other is drift-sonde operation.

In this study, we introduce a newly-developed, smaller, lighter, and cheaper upper-air radiosonde system designed with the capability of simultaneously receiving multiple weather systems. This so-called Storm Tracker system, developed at the Department of Atmospheric Sciences at National Taiwan University, has been tested in several field experiments since 2016. In section 2, the configuration of the Storm Tracker system is described in detail. Trial runs of preliminary comparisons between the Storm Tracker and the Vaisala RS41-SGP radiosonde are discussed in section 3. Section 4 concludes the current status of the Storm Tracker system and its applications in different field campaigns. Section 5 is the concluding remarks.

2. Configuration for Storm Tracker Upper-air Observation System

The Storm Tracker upper-air observation system is described in this section, which consists of the upper-air radiosonde (the Storm Tracker) and the surface signal receiving unit (the Ground Receiver). Figure shows the system block diagram of the Storm Tracker system.

a. The Storm Tracker radiosonde

The Storm Tracker radiosonde is packed with sensors and supporting hardware, as shown in Figure . The main portion includes the ATMEGA328p microcontroller, the U-blox MAX7-Q GPS sensor, the Bosch BMP280 pressure sensor, the TE-Connectivity HTU21D temperature-humidity sensor, and the LoRa™ transmitter.

The main processor of the Storm Tracker is the Microchip ATMEGA328p microcontroller (Atmel Corporation 2015). The microcontroller processes all measurements from the sensors and sends them to the radio transmitter.

For the GPS module, the U-blox MAX-7Q is selected (U-Blox 2014). This GPS module provides the altitude and speed as well as the direction of the Storm Tracker. The overall GPS module possesses an accuracy of 2.0 m for horizontal position and 0.1 m/s for velocity (U-Blox 2014).

radiosondes, which is explicitly for high temporal resolution observations on mesoscale weather systems. This so-called Storm Tracker system, developed at the Department of Atmospheric Sciences at National Taiwan University, has been tested in several field experiments since 2016. In section 2, the configuration of the Storm Tracker system is described in detail. Trial runs of preliminary comparisons between the Storm Tracker and the Vaisala RS41-SGP radiosonde are discussed in section 3. Section 4 concludes the current status of the Storm Tracker system and its applications in different field campaigns. Section 5 is the concluding remarks.

2. Configuration for Storm Tracker Upper-air Observation System

The Storm Tracker upper-air observation system is described in this section, which consists of the upper-air radiosonde (the Storm Tracker) and the surface signal receiving unit (the Ground Receiver). Figure 1 shows the system block diagram of the Storm Tracker system.

a. The Storm Tracker radiosonde

The Storm Tracker radiosonde is packed with sensors and supporting hardware, as shown in Figure 2. The main portion includes the ATMEGA328p microcontroller, the U-blox MAX7-Q GPS sensor, the Bosch BMP280 pressure sensor, the TE-Connectivity HTU21D temperature-humidity sensor, and the LoRa™ transmitter.

The main processor of the Storm Tracker is the Microchip ATMEGA328p microcontroller (Atmel Corporation 2015). The microcontroller processes all measurements from the sensors and sends them to the radio transmitter.

For the GPS module, the U-blox MAX-7Q is selected (U-Blox 2014). This GPS module provides the altitude and speed as well as the direction of the Storm Tracker. The overall GPS

The pressure sensor on the Storm Tracker is Bosch BMP280, with an overall operation range from 1100 to 300 hPa and from –40 to 85ºC, in addition to a typical accuracy of ±1hPa (Bosch Sensortec 2018). This sensor has been applied widely to indoor navigation, where a precise pressure measurement is required.

For the sensor of temperature (T) and relative humidity (RH), we used the HTU21D, a digital relative humidity sensor with temperature output from TE Connectivity. This sensor is chosen regarding its high accuracy (±0.3ºC in T and ±2% in RH), wide operational range (–40 to 125ºC, 0–100%), the short response time (5 seconds), and cutting-edge energy-saving property (TE Connectivity 2017). The HTU21D sensor is located at the 3-cm arm, as shown in Figure , to extend outside of the protection box to measure the environment. Table 3 briefly summarizes the operational ranges and typical accuracies of atmospheric measurements for the Storm Tracker and the Vaisala RS41-SGP radiosonde (VAISALA Corporation 2017).

The power for Storm Tracker comes from one AAA battery, and this minimizes the total weight. The radio transmitter is powered by LoRa™, which is a long-range, low-power wide-area network technology (Augustin et al. 2016). The radio frequency used by Storm Tracker ranges from 432MHz to 436.5MHz, the configuration for LoRa™ is 7 for spreading factor (SF) and 4/5 for code rate (CR) with 125kHz channel bandwidth. SF and CR, along with the channel bandwidth, define the transmission speed. Specifically, SF indicates the system's ability to receive the signal with a low Signal-to-Noise Ratio; the larger the number, the higher the sensitivity. For the Storm Tracker system, we set the SF to the lowest number of 7 in order to speed up the baud rate and make it enough for the communication range ~100km. Lastly, to extend the battery life to several hours, the transmit power is set to 18 dB with 1 Hz of transmission frequency.

As for the Storm Tracker enclosure, we use thick white paper with anti-water coating. Facing the temperature and humidity solar radiation biases found during the trial runs in 2017, module possesses an accuracy of 2.0 m for horizontal position and 0.1 m/s for velocity (U-Blox 2014).

The pressure sensor on the Storm Tracker is Bosch BMP280, with an overall operation range from 1100 to 300 hPa and from –40 to 85°C, in addition to a typical accuracy of ±1hPa (Bosch Sensortec 2018). This sensor has been applied widely to indoor navigation, where a precise pressure measurement is required.

For the sensor of temperature (T) and relative humidity (RH), we used the HTU21D, a digital relative humidity sensor with temperature output from TE Connectivity. This sensor is chosen regarding its high accuracy (±0.3°C in T and ±2% in RH), wide operational range (–40 to 125°C, 0–100%), the short response time (5 seconds), and cutting-edge energy-saving property (TE Connectivity 2017). The HTU21D sensor is located at the 3-cm arm, as shown in Figure 2, to extend outside of the protection box to measure the environment. Table 1 briefly summarizes the operational ranges and typical accuracies of atmospheric measurements for the Storm Tracker and the Vaisala RS41-SGP radiosonde (VAISALA Corporation 2017).

The power for Storm Tracker comes from one AAA battery, and this minimizes the total weight. The radio transmitter is powered by LoRa™, which is a long-range, low-power wide-area network technology (Augustin et al. 2016). The radio frequency used by Storm Tracker ranges from 432MHz to 436.5MHz, the configuration for LoRa™ is 7 for spreading factor (SF) and 4/5 for code rate (CR) with 125kHz channel bandwidth. SF and CR, along with the channel bandwidth, define the transmission speed. Specifically, SF indicates the system's ability to receive the signal with a low Signal-to-Noise Ratio; the larger the number, the higher the sensitivity. For the Storm Tracker system, we set the SF to the lowest number of 7 in order to speed up the baud rate, but still able to maintain the communication range to ~100km. Lastly, to extend the battery life, the transmit power is set to 18 dB with 1 Hz of transmission frequency. The resulted battery power can last for 2–4 hours.

we design a 1-mm thick tinplate metal shield to cover the temperature and humidity sensors to prevent direct solar radiation. The detail of the metal shield added to the Storm Tracker sonde is shown in Figure . The complete package of the Storm Tracker and the enclosure with the metal shield is shown in Figure 4.

For the production, a local printed circuit board (PCB) assembly factory manages the production of both the Storm Tracker and the Ground Receiver. The final cost of each Storm Tracker sonde (~50 USD) is about one-tenth of the price of a regular Vaisala RS41-SGP radiosonde as purchased in Taiwan.

Furthermore, since the Storm Tracker only weighs about 20g, including a battery, it can be easily carried by a constant volume foil balloon for constant-height flight, or pilot rubber balloon for regular upper-air observation. Figure 5 shows a typical Storm Tracker launch with a pilot rubber balloon, and Table 4 summarizes the Storm Tracker properties.

b. The Ground Receiver

We also designed a ground receiver to receive and process the data from Storm Tracker, the right panel of Figure 1 shows the system block diagram of the ground receiver. The RF module, as shown by the green block, will capture the incoming RF (Radio Frequency) signal, and we use the same RF module for Storm Tracker as the receiver. The package will then be sent to MCU for data parsing before being sent to the MPU (Main Processing Unit). The MCU we choose is the same as Storm Tracker (ATMEGA328p), and the MPU is a WiFi capable MT7688 SoC (System on Chip). MPU hosts the Web server and records the data to the external micro SD card. The power source can be either a USB power supply or a wide range of DC power supply (3~16 Volt) through DC Jack. Figure 6 shows a complete set of Storm Tracker Ground Receiver installed in a 3D-printed box (9cm*2cm*5cm). The Ground Receiver is then connected to an omnidirectional antenna with 6dB gain. A typical setup of the Ground Receiver in the field is shown in Figure 7.

As for the Storm Tracker enclosure, we use thick white paper with a water-proof coating. Facing the temperature and humidity solar radiation biases found during the trial runs in 2017, we design a 1-mm thick tinplate metal shield to cover the temperature and humidity sensors outside of the paper enclosure to prevent direct solar radiation. A detailed picture of the metal shield added to the Storm Tracker radiosonde is shown in Figure 3. The complete package of the Storm Tracker and the enclosure with the metal shield is shown in Figure 4.

For the production, a local printed circuit board (PCB) assembly factory manages the production of both the Storm Tracker and the Ground Receiver. The final cost of each Storm Tracker sonde is about ~50 USD.

Furthermore, since the Storm Tracker only weighs about 20g, including a battery, it can be easily carried by a constant volume foil balloon for constant-height flight, or pilot rubber balloon for regular upper-air observation. Figure 5 shows a typical Storm Tracker launch with a pilot rubber balloon, and Table 2 summarizes the Storm Tracker properties.

b. The Ground Receiver

A ground receiver was also designed to receive and process the data from the Storm Tracker radiosondes. The right panel of Figure 1 shows the system block diagram of the ground receiver. The radiofrequency (RF) module, as shown by the green block, will capture the incoming radio signal. The RF modules on the Storm Tracker radiosonde and the Ground Receiver are the same. The package will then be sent to the Micro Controller Unit (MCU) for data parsing before being sent to the MPU (Main Processing Unit). The MCU we choose is the same as Storm Tracker (ATMEGA328p), and the MPU is a WiFi capable MT7688 SoC (System on Chip). MPU hosts the Web server and records the data to the external micro SD card. The power supply for the Ground Receiver can be either a USB power supply or a wide range of DC power supply (3~16 Volt) through DC Jack. Figure 6 shows a complete set of Storm Tracker Ground Receiver installed in a 3D-printed box (9cm*2cm*5cm). The Ground

The most powerful feature of the Storm Tracker system is the ability to receive data from up to ten radiosondes simultaneously, which provides the opportunity of upper-air observations with extremely high temporal/spatial resolution. In a word, one can launch up to ten Storm Trackers at once with only a receive; or launch a series of Storm Trackers in a short period, say an hour, 30 minutes, or even 10 minutes depending on the mission.

To accomplish this goal with a single-channel transceiver on the Storm Tracker, time-divided multi-access (TDMA) was implemented into the Storm Tracker system. Since each Storm Tracker takes about 76ms for data transmission, the system splits every second into 10-time slots, and each Storm Tracker transmits the data on the different time slots pre-assigned during Storm Tracker manufacture programming. Therefore, the Ground Receiver is constantly scanning ten different frequencies per second and tracking up to ten Storm Trackers at the same time.

A newer version of the Ground Receiver is currently underway, which is powered by Raspberry Pi and a unique in-house designed LoRa™ gateway, which can receive 8-channel simultaneously. In the future, this new design with TDMA could monitor 80 Storm Trackers at the same time.

c. The launch procedure

Nevertheless, the Storm Tracker system is still under development and testing. Here we present the launch and ground check procedure for the latest intercomparison field experiment. First, we install the battery and place the Storm Tracker at a location that it can receive the GPS signal. Once the GPS signal has been received, the data will be transmitted and show up on the receiver's webpage. The user can check if the measurements are correct as in other radiosonde launching processes, such as the Storm, Tracker ID number, battery voltage, and the instrument data. The Storm Tracker is then clear to launch.

Receiver is then connected to an omnidirectional antenna with a 6dB gain. A typical setup for the Ground Receiver outside in the field is shown in Figure 7.

The most powerful feature of the Storm Tracker system is the ability to receive data from up to ten radiosondes simultaneously, which provides the opportunity for upper-air observations with extremely high temporal/spatial resolution. In a word, one can launch up to ten Storm Trackers at once with only one receiver; or launch a series of Storm Trackers on a very short time interval, say hourly, every 30 minutes, or even every 10 minutes depending on the mission.

To accomplish this goal with a single-channel transmitter on the Storm Tracker, time-divided multi-access (TDMA) technology was implemented into the Storm Tracker system. Since each Storm Tracker takes about 76ms for data transmission, the system splits every second into 10-time slots, and each Storm Tracker transmits the data on the different time slots pre-assigned during Storm Tracker manufacture programming. In practice, the Ground Receiver is constantly scanning ten different frequencies per second and tracking up to ten Storm Trackers at the same time.

A newer version of the Ground Receiver is currently underway, which is powered by Raspberry Pi and a unique in-house designed LoRa™ gateway, which can receive 8-channel simultaneously. In the future, this new design with TDMA could monitor 80 Storm Trackers at the same time.

c. The launch procedure

Numerous developing processes and tests are still needed for the Storm Tracker system. Here we present the launch and ground check procedure for the latest intercomparison field experiment. First, we install the battery and place the Storm Tracker at a location where it can receive the GPS signal from satellites. Once the GPS signal has been received, the data will be transmitted and show up on the receiver's webpage. The user can check if the measurements

The overall setup of the Storm Tracker system before the actual launch is relatively easy and takes less amount of time (~10 min) comparing to a regular Vaisala ground system. This also shortens the preparation time for the observation of short-term weather events such as thunderstorms.

3. The intercomparison between the Storm Tracker and Vaisala RS41-SGP

a. Field experiment design

Two trial field experiments were conducted to examine the performance of the Storm Tracker system on the boundary layer (BL) observations. In these trial runs, we attached the Storm Tracker to the side of RS41-SGP by double-sided foam tape, with the sensor arm of Storm Tracker sticking out from the main body, as shown in Figure 8. The first trial run was conducted for four days in December 2017 at Wu-Chi, Taichung, Taiwan, and in total 28 sets of Storm Tracker and Vaisala RS41 were launched. One of the results from this trial run is the solar radiation affecting the temperature and moisture measurements. Therefore, we installed a thin metal shell (i.e., the "hat") around the temperature/humidity sensor, as shown in Figure , to prevent the direct solar heating in the second trial run conducted at the same location in July 2018. During the second run, every launch includes a Vaisala RS41 attached with two Storm Trackers, one with and one without the hat. Similar to the first run, the data from 19 co-launches under the clear sky were collected, the average vertical profile from the Vaisala RS41 shows a clear signature of subsidence and an overall dry atmosphere (Figure 9). In this section, the data from the second run will be shown to examine the performance by adding the metal shield.

b. Humidity time-lag error analysis

Since both the Storm Tracker and the Vaisala RS41-SGP transmit data every second, we could first analyze the time lag error for humidity. The analysis is done by separating the time-series data into three different altitude sections: 200m to 3000m, 3000m to 4500m and > 4500m. For each section of the time-series, we find the resulting delay that maximizes the are stable as well as other parameters such as the Storm Tracker ID number and battery voltage. The Storm Tracker is then clear to launch.

The overall setup of the Storm Tracker system before the actual launch is relatively easy and takes less amount of time (~10 min) comparing to a regular Vaisala ground system. This also shortens the preparation time for the observation of short-term weather events such as an afternoon thunderstorm.

3. The intercomparison between the Storm Tracker and Vaisala RS41-SGP

a. Field experiment design

Two trial field experiments were conducted to examine the performance of the Storm Tracker system on the boundary layer (BL) observations. In these trial runs, we attached the Storm Tracker to the side of Vaisala RS41-SGP by double-sided foam tape, with the sensor arm of Storm Tracker sticking out from the main body, as shown in Figure 8. The first trial run was conducted for four days in December 2017 at Wu-Chi, Taichung, Taiwan, and in total 28 sets of Storm Tracker and Vaisala RS41 were launched. One of the results from this trial run is the solar radiation affecting the temperature and moisture measurements. Therefore, we installed a thin metal shell (i.e., the "hat") around the temperature/humidity sensor, as shown in Figure 3, to prevent the direct solar heating in the second trial run conducted at the same location in July 2018. During the second run, every launch includes a Vaisala RS41 attached with two Storm Trackers, with and without the hat. Similar to the first run, the data from 19 co-launches under the clear sky were collected, the average vertical profile from the Vaisala RS41 shows a clear signature of subsidence and an overall dry atmosphere (Figure 9). In this section, the data from the second run will be shown to examine the effects of adding the metal shield.

The overall vertical profile data collected during this experiment is shown in Figure 10. It is similar to Figure 2 and 3 of Fujiwara et al. (2003), which shift each vertical profile cross-correlation. To exclude the effect of solar radiation heating, we use only the nighttime data to calculate the time-lag. The average time-lags are shown in Table 4.

One example of the time-series is shown in Figure 11. We could see that for humidity without the metal shield, the time lag is about 5 to 8 seconds. And the higher the altitude, the longer the time-lag. Furthermore, in the case of adding the metal shield, the time-lag is longer compared to the case without a metal shield, which indicates that the metal shield might affect the ventilation, but overall the time-lag is still small around 7 to 9 seconds.

c. Temperature and humidity solar radiation biases analysis

The raw data from both Storm Tracker and Vaisala RS41-SGP were analyzed by calculating the difference along with the time series. For calculating the mean and standard deviation of the biases across different altitudes, the Vaisala RS41 altitude data was used as the reference, and the vertical profiles are from 200m to 6000m at a 20m interval. The data during daytime (8–18 LST) and nighttime (18–8 LST) were separated to see how the sensor response to solar radiation. The vertical profiles of Temperature and Humidity biases are shown in Figure 10, and the statistics are in Table 3.

First, we can see from Figure 10(a) that either with or without the metal shield, the temperature, and humidity sensor had experienced significant solar heating during the daytime, which also caused the solar radiation dry bias (Vömel et al. 2007) in moisture measurements. Furthermore, temperature bias increases with altitude. Overall, with the metal shield added, the standard deviation and mean of the biases are smaller at most altitudes (Figure 10(c)). As shown in Table 3, during the daytime, the mean temperature warm bias drops from 2.98ºC to 2.61ºC by adding the hat. The standard deviation also drops from 1.61ºC to 1.23ºC. Likewise, the mean dry bias drops from 3.47% drier to 2.43% drier with the hat. Moreover, the standard deviation decreases from 6.44% to 5.3%. These results show that the reflective metal shield does help to prevent direct solar heating when the Storm Tracker is in the air.

according to the launch time and plot all the vertical profiles. Here we added 2% per hour to humidity data, 2 °C per hour for temperature data, 2 m/s per hour for Wind data. According to Figure 10, the Storm Trackers could measure properly at least up to 5000m high, and perform overall good agreement among each Storm Trackers. In addition, we also present one of the time series comparisons between the Storm Tracker and the Vaisala RS41-SGP in Figure 11. According to Figure 11, the Storm Tracker shows high consistency with the RS41-SGP, especially in the pressure and wind measurements. Slight lags were found in temperature and humidity measurements, which will be discussed in the following section.

b. Humidity time-lag error analysis

Since both the Storm Tracker and the Vaisala RS41-SGP transmit data every second, we could first analyze the time lag error for humidity. The analysis is done by separating the time-series data into three different altitude sections: 200m to 3000m, 3000m to 4500m and > 4500m. For each section of the time-series, we find the resulting delay that maximizes the cross-correlation. To exclude the effect of solar radiation heating, we use only the nighttime data to calculate the time-lag. The average time-lags are shown in Table 4.

One example of the time-series is shown in Figure 12. We could see that for the humidity measurements without the metal shield, the time lag is about 5 to 8 seconds. And the higher the altitude, the longer the time-lag. Furthermore, in the case of adding the metal shield, the time-lag is longer compared to the case without a metal shield, which indicates that the metal shield might affect the ventilation, but overall the time-lags are still within an acceptable range of 7 to 9 seconds. According to the results, the time-lag correction is omitted at this stage of analyses.

c. Temperature and humidity solar radiation biases analysis

The raw data from both Storm Tracker and Vaisala RS41-SGP were analyzed by calculating the difference along with the time series. For calculating the mean and standard

However, the installation of the metal shield causes a further warm bias when there is no solar heating. From Figure 10(b), we can see that the case with the metal shield experienced a warm bias in the profile, which also caused the humidity moist bias to drop and brought down the overall humidity difference. In Table 3, the mean warm bias increases from 0.16ºC without the hat to 1.29ºC with the hat, and the standard deviation increases from 0.39ºC to 0.54ºC. The mean humidity bias, on the other hand, drops from 5.63% moister for Storm Tracker without the hat to 1.82% for Storm Tracker with the hat. In both cases, the standard deviation is similar ~3.5%. During the nighttime, the results show that the metal shield further induces a warm bias, which may be the leading cause of the drying moist bias.

Finally, we look at Figure 10(c), and we can see the benefit of lowering the variances of measurements by adding the metal shield onto the temperature/humidity sensor. In Table 3, on average, even though mean warm bias increases from 1.52ºC to 1.93ºC if the hat is added, the standard deviation decreases from 1.82ºC to 1.15ºC. Moreover, the mean humidity bias improves from 1.23% to -0.23% with the hat, and the standard deviation also drops from 6.84% to 4.92% with the hat.

Even though the metal shield causes a slight warm bias during the nighttime, it mitigates the solar radiation heating effects and the solar radiation dry bias during the daytime when most of the mesoscale convective rainfall occurs. For such events in Taiwan, it is worthwhile to apply these new instruments to acquire much higher resolution data, especially for afternoon thunderstorms triggered by daytime solar heating.

d. Pressure and GPS analysis

Since the Vaisala RS41-SGP is equipped with a pressure sensor, we also compared our BMP280 sensor with that of the Vaisala RS41-SGP, as shown in Table 5. Although the resulting initial error is higher than BMP280's accuracy, we tried to mitigate the difference by applying a ground check procedure on the pressure measurements for each launch. As indicated deviation of the biases across different altitudes, the Vaisala RS41 altitude data was used as the reference, and the vertical profiles are from 200m to 6000m at a 20m interval. The data during daytime (8–18 LST) and nighttime (18–8 LST) were separated to see how the sensor response to solar radiation. The vertical profiles of Temperature and Humidity biases are shown in Figure 13, and the statistics are in Table 3.

First, we can see from Figure 13(a) that either with or without the metal shield, the temperature and humidity sensor had experienced significant solar heating during the daytime, which also caused the solar radiation dry bias (Vömel et al. 2007) in moisture measurements. Furthermore, temperature bias increases with altitude. Overall, with the metal shield added, the standard deviation and mean of the biases are smaller at most altitudes, as shown in Figure 13(c). As shown in Table 3, during the daytime, the mean temperature warm bias drops from 2.98ºC to 2.61ºC by adding the hat. The standard deviation also drops from 1.61ºC to 1.23ºC. Likewise, the mean dry bias drops from 3.47% drier to 2.43% drier with the hat. Moreover, the standard deviation decreases from 6.44% to 5.3%. These results show that the reflective metal shield does help to prevent direct solar heating when the Storm Tracker is in the air.

However, the installation of the metal shield causes a further warm bias when there is no solar heating. From Figure 13(b), we can see that the case with the metal shield experienced a warm bias in the profile, which also caused the humidity moist bias to drop and brought down the overall humidity difference. In Table 3, the mean warm bias increases from 0.16ºC without the hat to 1.29ºC with the hat, and the standard deviation increases from 0.39ºC to 0.54ºC. The mean humidity bias, on the other hand, drops from 5.63% moister for Storm Tracker without the hat to 1.82% for Storm Tracker with the hat. In both cases, the standard deviation is similar ~3.5%. During the nighttime, the results show that the metal shield further induces a warm bias, which may be the leading cause of the drying moist bias.

in Table 5, the resulted pressure measurements were further improved that the mean pressure error drops from 2.76 hPa to 0.33 hPa for Storm Tracker without the hat, and the trend is the same for Storm Tracker with the hat. In addition, for the measurements derived for the GPS, the Storm Tracker performs very well comparing to the Vaisala RS41-SGP, as shown in Table 5.

4. Applications in the field campaigns

One of the main scientific purposes of the experiments conducted is to examine the performance of the Storm Tracker system on the BL observations. In Figure 12, we present the time-height series data across the experiment timeline. The colors represent θ_e, and the arrow represents the wind speed and direction. The BL heights (gray lines) were calculated according to the method described in Liu and Liang (2010). Here we can see that the evolution of the boundary layer grows and maximized near noon. Moreover, with the higher temporal resolution of ~3-hourly, we could see the diurnal cycle of the development of the boundary layer. This demonstrates one of the use cases for Storm Tracker in gathering high temporal or spatial data enabled by the ability of simultaneous signal receiving.

Another campaign during typhoon Talim on September 13, 2017, was conducted with three Storm Trackers to see if the observations inside the tropical cyclones are possible. As shown in Figure 13, light-weighted Storm Tracker can be launched with a conventional and small constant balloon, which then can stay afloat at a fixed atmospheric layer. Figure 13 shows the flight path and the altitude of the Storm Tracker into the typhoon. In this experiment, the Storm Tracker stayed at 6200m for about 1 hour. Although the signal was lost eventually by the mountains blocking between the receiver and the Storm Tracker, this launch shows the potential of Storm Tracker to conduct drift sound experiments in the future.

5. Concluding remarks

Finally, in Figure 13(c), we can see the benefit of lowering the variances of measurements by adding the metal shield onto the temperature/humidity sensor. In Table 3, on average, even though the mean warm bias increases from 1.52ºC to 1.93ºC with the hat added, the standard deviation decreases from 1.82ºC to 1.15ºC. Moreover, the mean humidity bias improves from 1.23% to -0.23% with the hat, and the standard deviation also drops from 6.84% to 4.92% with the hat.

Even though the metal shield causes a warm bias during the nighttime, it mitigates the solar radiation heating effects and the solar radiation dry bias during the daytime when most of the severe weather occurs. For such events in Taiwan, it is worthwhile to apply these new instruments to acquire much higher resolution data, especially for afternoon thunderstorms triggered by daytime solar heating.

d. Pressure and GPS analysis

Since the Vaisala RS41-SGP is equipped with a pressure sensor, we also compared our BMP280 sensor with that of the Vaisala RS41-SGP, as shown in Table 5. Although the resulting initial error is higher than BMP280's accuracy, we tried to mitigate the difference by applying a ground check procedure on the pressure measurements for each launch. As indicated in Table 5, the pressure measurement result was further improved that the mean pressure error drops from 2.76 (2.59) hPa to 0.33 (0.43) hPa for Storm Tracker without (with) the hat. In addition, for the measurements derived from the GPS sensor, the Storm Tracker performs very well comparing to the Vaisala RS41-SGP.

4. Applications in the field campaigns

One of the main scientific purposes of the experiments conducted is to examine the performance of the Storm Tracker system on the BL observations. In Figure 14, we present the time-height series data across the experiment timeline. The colors represent θ_e (equivalent potential temperature), and the arrow represents the wind speed and direction. The BL heights

Although the Storm Tracker system is incorporated with the new low-cost sensors, we show that it can accomplish decent performance compared with Vaisala RS41 radiosonde with a significant cost reduction. Moreover, with the capability of tracking multi-tracker simultaneously and incorporating LoRa™ technology, it enables future missions to deploy many radiosondes to collect higher temporal/spatial resolution data.

These trial runs show that the Storm Tracker radiosondes still have issues regarding temperature and moisture measurements. Still, the current configuration with a thin metal shield does help with the daytime biases and lowering the variance. More experiments to compare the measurements between the Storm Tracker and Vaisala RS41 are underway, in addition to the intercomparison among different individual instruments such as radiometer. More importantly, with more intercomparison data, the objective correction algorithms are currently developed and tested for better data quality control.

Data availability

All field measurement data from our Storm Tracker and Vaisala RS-41-SGP could be accessed through FTP by request.

Authors contribution

Mr. Hwang makes the PCB, program coding, and document draft. Dr. Lin supports all funding of this study and coordinated field tests. Dr. Yu joins the discussion of data intercomparison.

Competing interests

The authors declare that they have no conflict of interest.

Acknowledgments

The authors would like to thank the RS-41 data sharing from RCEC (Research Center for Environmental Changes) in Academia Sinica, and the field test supported by TASSE program (MOST 108-2119-M-002-022) which is managed by Prof. Hung-Chi Kuo, National Taiwan

(gray lines) were calculated according to the method described in Liu and Liang (2010), which is mainly based on the vertical profiles of θ_e and wind speeds. During the 2018 trial run, the overall Taiwan area is dominated by the subtropical high, resulting in the subsidence, as seen in Figure 9 and relatively clear weather (Figure 15).

Here we can see that the evolution of the boundary layer grows and maximized near noon. Moreover, with the higher temporal resolution of up to 3-hourly, we could see the diurnal cycle of the development of the boundary layer. This demonstrates one of the use cases for the Storm Tracker in gathering high temporal or spatial data enabled by the ability of simultaneous signal receiving.

Another campaign during typhoon Talim on September 13, 2017, was conducted with three Storm Trackers to see if the observations within the tropical cyclones are possible (the tracks are shown in Figure 16). The light-weighted Storm Tracker can be launched with a conventional and small constant balloon, which then can stay afloat at a fixed altitude. Figure 17 shows the time-series instrument data of the Storm Tracker 0. In this experiment, the Storm Tracker stayed at about 6200m. Although the signal was lost eventually by the mountains blocking between the Ground Receiver and the Storm Tracker, this launch shows the potential of Storm Tracker to conduct drift sound experiments in the future.

5. Concluding remarks

Although the Storm Tracker system is incorporated with the new low-cost sensors, we show that it can accomplish decent performance compared with Vaisala radiosondes with a significant cost reduction. Moreover, with the capability of tracking multi-tracker simultaneously and incorporating LoRa™ technology, it enables future missions to deploy many radiosondes to collect higher temporal/spatial resolution data.

These trial runs show that the Storm Tracker radiosondes still have issues regarding temperature and moisture measurements. Still, the current configuration with a thin metal

shield does help with the daytime biases and lowering the variance. More experiments to compare the measurements between the Storm Tracker and Vaisala RS41 are underway, in addition to the intercomparison among different individual instruments such as radiometer. More importantly, with more intercomparison data, the objective correction algorithms are currently developed and tested for better data quality control.

Data availability

All field measurement data from our Storm Tracker and Vaisala RS-41-SGP could be accessed through FTP by request.

Authors contribution

Mr. Hwang makes the PCB, program coding, and document draft. Dr. Lin supports all funding of this study and coordinated field tests. Dr. Yu joins the discussion of data intercomparison.

Competing interests

The authors declare that they have no conflict of interest.

Acknowledgments

The authors would like to thank the RS-41 data sharing from RCEC (Research Center for Environmental Changes) in Academia Sinica, and the field test supported by TASSE program (MOST 108-2119-M-002-022) which is managed by Prof. Hung-Chi Kuo, National Taiwan University. We also appreciate the efforts of the associate editor and the anonymous reviews whose comments to improve this paper

University. We also appreciate the efforts of the associate editor and the anonymous reviews whose comments to improve this paper

References

Atmel Corporation, 2015: ATmega328P 8-bit AVR Microcontroller with 32K Bytes In-System Programmable Flash Datasheet. ATmega328P [DATASHEET] 7810D–AVR–01/15, 294 pp, http://ww1.microchip.com/downloads/en/DeviceDoc/Atmel-7810-Automotive-Microcontrollers-ATmega328P_Datasheet.pdf.

Augustin, A.; Yi, J.; Clausen, T.; Townsley, W.M., 2016: A Study of LoRa: Long Range & Low Power Networks for the Internet of Things. Sensors, 16, 1466. https://doi.org/10.3390/s16091466.

Bosch Sensortec, 2018: Datasheet BMP280 Digital Pressure Sensor. BST-BMP280-DX001-19, 49 pp, https://ae-bst.resource.bosch.com/media/_tech/media/datasheets/BST-BMP280-DS001.pdf.

Fujiwara, M., S.-P. Xie, M. Shiotani, H. Hashizume, F. Hasebe, H. Vömel, S. J. Oltmans, and T. Watanabe (2003),Upper-tropospheric inversion and easterly jet in the tropics,Journal of Geophysical Research, 108, No. D24, 2796, doi: 10.1029/2003JD003928.

Ingleby, B.,2017: An assessment of different radiosonde types 2015/2016. ECMWF Technical Memoranda, 807. Pp77.

MediaTek, 2016: MediaTek MT7688 Datasheet, 294 pp, http://labs.mediatek.com/en/chipset/MT7688

Nash, J., Oakley, T., Vömel, H., & Wei, L., 2011: WMO intercomparison of high quality radiosonde systems, Yangjiang, China, 12 July–3 August 2010. World Meteorological Organization, Instruments and Observing methods, report No, 107.

TE Connectivity, 2017: HTU21D(F) RH/T SENSOR IC Digital Relative Humidity sensor with Temperature output. HTU21D(F) RH/T SENSOR IC, 22pp, https://www.te.com/commerce/DocumentDelivery/DDEController?Action=showdoc

References

Atmel Corporation, 2015: ATmega328P 8-bit AVR Microcontroller with 32K Bytes In-System Programmable Flash Datasheet. ATmega328P [DATASHEET] 7810D–AVR–01/15, 294 pp, http://ww1.microchip.com/downloads/en/DeviceDoc/Atmel-7810-Automotive-Microcontrollers-ATmega328P_Datasheet.pdf.

Augustin, A.; Yi, J.; Clausen, T.; Townsley, W.M., 2016: A Study of LoRa: Long Range & Low Power Networks for the Internet of Things. Sensors, 16, 1466. https://doi.org/10.3390/s16091466.

Bosch Sensortec, 2018: Datasheet BMP280 Digital Pressure Sensor. BST-BMP280-DX001-19, 49 pp, https://ae-bst.resource.bosch.com/media/_tech/media/datasheets/BST-BMP280-DS001.pdf.

Ingleby, B.,2017: An assessment of different radiosonde types 2015/2016. ECMWF Technical Memoranda, 807. Pp77.

MediaTek, 2016: MediaTek MT7688 Datasheet, 294 pp, http://labs.mediatek.com/en/chipset/MT7688

Nash, J., Oakley, T., Vömel, H., & Wei, L., 2011: WMO intercomparison of high quality radiosonde systems, Yangjiang, China, 12 July–3 August 2010. World Meteorological Organization, Instruments and Observing methods, report No, 107.

TE Connectivity, 2017: HTU21D(F) RH/T SENSOR IC Digital Relative Humidity sensor with Temperature output. HTU21D(F) RH/T SENSOR IC, 22pp, https://www.te.com/commerce/DocumentDelivery/DDEController?Action=showdoc&DocId=Data+Sheet%7FHPC199_6%7FA6%7Fpdf%7FEnglish%7FENG_DS_HPC199_6_A6.pdf%7FCAT-HSC0004.

&DocId=Data+Sheet%7FHPC199_6%7FA6%7Fpdf%7FEnglish%7FENG_DS_HPC199_6_A6.pdf%7FCAT-HSC0004.

U-Blox, 2014: MAX-7 u-blox 7 GNSS modules Data Sheet. UBX-13004068, 24 pp, https://www.u-blox.com/sites/default/files/products/documents/MAX-7_DataSheet_%28UBX-13004068%29.pdf.

VAISALA Corporation, 2017: Vaisala Radiosonde RS41-SGP. B211444EN-E, 2pp, https://www.vaisala.com/sites/default/files/documents/WEA-MET-RS41SGP-Datasheet-B211444EN.pdf.

Vömel, H., H. Selkirk, L. Miloshevich, J. Valverde-Canossa, J. Valdes, E. Kyrö, R. Kivi, W. Stolz, G. Peng, and J. A. Diaz (2007), Radiation dry bias of the Vaisala RS92 humidity sensor, J. Atmos. Oceanic Technol., 24, 953âAŠ963.

Shuyan , Liu, and Liang Xin-Zhong. “Observed Diurnal Cycle Climatology of Planetary Boundary Layer Height.” Journal of Climate, vol. 23, 2010, pp. 5790–5809., doi:10.1175/2010JCLI3552.1.

U-Blox, 2014: MAX-7 u-blox 7 GNSS modules Data Sheet. UBX-13004068, 24 pp, https://www.u-blox.com/sites/default/files/products/documents/MAX-7_DataSheet_%28UBX-13004068%29.pdf.

VAISALA Corporation, 2017: Vaisala Radiosonde RS41-SGP. B211444EN-E, 2pp, https://www.vaisala.com/sites/default/files/documents/WEA-MET-RS41SGP-Datasheet-B211444EN.pdf.

Vömel, H., H. Selkirk, L. Miloshevich, J. Valverde-Canossa, J. Valdes, E. Kyrö, R. Kivi, W. Stolz, G. Peng, and J. A. Diaz (2007), Radiation dry bias of the Vaisala RS92 humidity sensor, J. Atmos. Oceanic Technol., 24, 953âAŠ963.

Shuyan , Liu, and Liang Xin-Zhong. “Observed Diurnal Cycle Climatology of Planetary Boundary Layer Height.” Journal of Climate, vol. 23, 2010, pp. 5790–5809., doi:10.1175/2010JCLI3552.1.

Caption List

Table 1. List of the operational ranges and typical accuracies of basic atmospheric measurements for Vaisala RS41-SGP radiosonde (VAISALA Corporation 2017) and the Storm Tracker.

Table 2. Characteristics of Storm Tracker.

Table 3. Temperature and Humidity Error (Storm Tracker minus Vaisala RS41-SGP) Statistics for the second intercomparison experiment in July 2018 at Wu-Chi.

Table 4. Average time-lag for the second intercomparison experiment in July 2018 at Wu-Chi.

Table 5. All the sensor error (Storm Tracker minus Vaisala RS41-SGP) statistics for the second intercomparison experiment in July 2018 at Wu-Chi.

Figure 1. System block diagram for the Storm Tracker system, including Storm Tracker (left) and Receiver (right). The part number for the chipset is indicated in the box, and the arrow indicated the dataflow.

Figure 2. Photo of a PCB assembled Storm Tracker product from the PCBA. The diameter of the Storm Tracker is 58.1mm x 50.2mm (height x width, including sensor arm). The GPS antenna and GPS module are located on the top right of Storm Tracker, along with the power switching on the top left. The RF module is located on the bottom, and the red wire is the quarter-wave antenna. The extended arm hosts the temperature and humidity sensor, and the

Caption List

Table 1. List of the operational ranges and typical accuracies of basic atmospheric measurements for Vaisala RS41-SGP radiosonde (VAISALA Corporation 2017) and the Storm Tracker.

Table 2. Characteristics of Storm Tracker.

Table 3. Temperature and Humidity Error (Storm Tracker minus Vaisala RS41-SGP) Statistics for the second intercomparison experiment in July 2018 at Wu-Chi.

Table 4. Average time-lag for the second intercomparison experiment in July 2018 at Wu-Chi.

Table 5. All the sensor error (Storm Tracker minus Vaisala RS41-SGP) statistics for the second intercomparison experiment in July 2018 at Wu-Chi.

Figure 1. System block diagram for the Storm Tracker system, including Storm Tracker (left) and Receiver (right). The part number for the chipset is indicated in the box, and the arrow indicated the dataflow.

Figure 2. Photo of a PCB assembled Storm Tracker product from the PCBA. The diameter of the Storm Tracker is 58.1mm x 50.2mm (height x width, including sensor arm). The GPS antenna and GPS module are located on the top right of Storm Tracker, along with the power switch on the top left. The RF module is located on the bottom, and the red wire is the quarter-wave antenna. The extended arm hosts the temperature and humidity sensor, and the pins on

pins on the bottom are for programming and debug purposes. Lastly, in the middle are the microcontroller and pressure sensor.

Figure 3. A closeup picture of the metal shield. The metal shield is a 15mm x 15mm x 15mm square cube, and the inner sensor PCB is a 7mm x 7mm square.

Figure 4. A Storm Tracker with the enclosure and the metal shield. The enclosure is composed of paper, and the hole on the top (bottom) is for connecting to the balloon (passing of the antenna). The metal shield is attached to the PCB board with hot glue.

Figure 5. A Storm Tracker (without enclosure) launched with a pilot rubber balloon (20g) during a field campaign.

Figure 6. Photo of a Storm Tracker Ground Receiver. On the right are the GPS module and RF module to receive the signal, along with the USB and DC power jack for power input and the console access. In the middle is the central processor, which handles data recording and hosts the website. On the left is the SD card for storage. On the top are the indicator LEDs, which show the current status of the receiver and the received data channels.

Figure 7. A typical setup of the ground receiver in the field, with the 433Mhz antenna in the middle, and the receiver, GPS antenna and power bank at the bottom black box.

Figure 8. A photo of the intercomparison launch setup. The Storm Tracker is attached to the side of a Vaisala RS41 radiosonde with double side tape.

the bottom are for programming and debug purposes. Lastly, in the middle are the microcontroller and pressure sensor.

Figure 3. A closeup picture of the metal shield. The metal shield is a 15mm x 15mm x 15mm square cube, and the inner sensor PCB is a 7mm x 7mm square.

Figure 4. A Storm Tracker with the enclosure and the metal shield. The enclosure is composed of paper, and the hole on the top (bottom) is for connecting to the balloon (passing of the antenna). The metal shield is attached to the PCB board with hot glue.

Figure 5. A Storm Tracker (without enclosure) launched with a pilot rubber balloon (20g) during a field campaign.

Figure 6. Photo of a Storm Tracker Ground Receiver. On the right are the GPS module and RF module to receive the signal, along with the USB and DC power jack for power input and the console access. In the middle is the central processor, which handles data recording and hosts the website. On the left is the SD card for storage. On the top are the indicator LEDs, which show the current status of the receiver and the received data channels.

Figure 7. A typical setup of the ground receiver in the field, with the 433Mhz antenna in the middle, and the receiver, GPS antenna and power bank at the bottom black box.

Figure 8. A photo of the intercomparison launch setup. The Storm Tracker is attached to the side of a Vaisala RS41 radiosonde with double side tape.

Figure 9. The skew-T-log-P diagram of the average vertical profile measured by Vaisala RS41 radiosondes during the intercomparison run in July 2018 at Wu-Chi. The thick red line indicated the dew point, and the thick blue line indicated the temperature profile.

Figure 10. (a) top (b) middle (c) bottom The vertical profiles for temperature and humidity differences during both the daytime and nighttime in July 2018 at Wu-Chi experiment. The lines indicated the mean, and the one standard deviation ranges are shaded. The red color indicates daytime data, and blue color indicates nighttime data.

Figure 11. One of the launch data for time-lag analysis, the original time-series data, is at the top. And the time-lag corrected time-series in the middle, with three segments of the time series data for three altitude bins. And lastly, the altitude to time-lag plot at the bottom.

Figure 12. The time-series-height data for the experiment done during July 2018 at Wu-Chi. The shaded color represents $\boldsymbol{\theta_e}$ and the arrow direction indicates wind direction with length indicate the wind speed. Lastly, the gray line is the boundary height calculated with the algorithm developed by Liu and Liand in 2010.

Figure 13. Three balloon tracks during Typhoon Talim (top) and the height profile of the Storm Tracker 0 (bottom). The height profile at the bottom is the time series data with time at the x-axis and height(meter) at the y-axis. The launching site is located on the campus of National Taiwan University. The maximum range of the Storm Tracker from the site is 132km, in which the Storm Tracker could maintain at about 6200m height. Credit to Google Earth Pro for providing the satellite image.

Figure 9. The skew-T-log-P diagram of the average vertical profile measured by Vaisala RS41 radiosondes during the intercomparison run in July 2018 at Wu-Chi. The thick red line indicated the dew point, and the thick blue line indicated the temperature profile.

Figure 10. Temporal changes in the vertical profile during the intercomparison run in July 2018 at Wu-Chi. Each vertical profile was shifted according to the launch time. Here we added 2% per hour to humidity data, 2 °C per hour for temperature data, 2 m/s per hour for Wind data.

Figure 11. One of the time series comparisons during the intercomparison run in July 2018 at Wu-Chi. The blue line indicates Storm Tracker time-series data, and the orange line indicates RS41-SGP time series data.

Figure 12. One of the launch data for time-lag analysis, the original time-series data, is at the top. And the time-lag corrected time-series in the middle, with three segments of the time series data for three altitude bins. And lastly, the altitude to time-lag plot at the bottom. The time lag for this case is 2s (200~3000m), 4s (3000~4500m) and 4s (4500m up).

Figure 13. (a) top (b) middle (c). bottom The vertical profiles for temperature and humidity differences during both the daytime and nighttime in July 2018 at Wu-Chi experiment. The lines indicated the mean, and the one standard deviation ranges are shaded. The red color indicates daytime data, and blue color indicates nighttime data.

Figure 14. The time-series-height data for the experiment done during July 2018 at Wu-Chi. The shaded color represents $\boldsymbol{\theta_e}$ and the arrow direction indicates wind direction with length

indicate the wind speed. Lastly, the gray line is the boundary height calculated with the algorithm developed by Liu and Liand in 2010.

Figure 15. Synoptic chart during the experiment done during July 2018 at Wu-Chi. Credit to Central Weather Bureau for providing the Synoptic chart.

Figure 16. Three balloon tracks during Typhoon Talim (Red, yellow, and green tracks are Storm Tracker 0, 1, and 2). The launching site is located on the campus of National Taiwan University. The maximum range of the Storm Tracker from the site is 132km. Credit to Google Earth Pro for providing the satellite image.

Figure 17. Storm Tracker 0 time-series data during Typhoon Talim. The altitude of Storm Tracker can maintain at around 6200 meters.

Tables

Table 3. List of the operational ranges and typical accuracies of basic atmospheric measurements for Vaisala RS41-SGP radiosonde (VAISALA Corporation 2017) and the Storm Tracker.

Spec	Vaisala RS41-SGP	Storm Tracker
P Range	sfc. - 3 hPa	1100 - 300 hPa
P Accu.	1.0 hPa (>100 hPa)	1 hPa (0 - 65 ℃)
		1.7 hPa (-20 - 0 ℃)
T Range	-90 - +60 ℃	-40 - +125 ℃
T Accu.	0.3 ℃ (<16 km)	0.3 ℃
	0.4 ℃ (>16 km)	
RH Range	0 - 100 %	0 - 100 %
RH Accu.	4%	2%
Horizontal WIND SPEED Accu.	0.15 m/s	0.1 m/s
		(Hor. Accu.: 2.5 m)

Tables

Table 1. List of the operational ranges and typical accuracies of basic atmospheric measurements for Vaisala RS41-SGP radiosonde (VAISALA Corporation 2017) and the Storm Tracker.

Spec	**Vaisala RS41-SGP**	**Storm Tracker**
P Range	sfc. - 3 hPa	1100 - 300 hPa
P Accu.	1.0 hPa (>100 hPa)	1 hPa (0 - 65 ℃)
		1.7 hPa (-20 - 0 ℃)
T Range	-90 - +60 ℃	-40 - +125 ℃
T Accu.	0.3 ℃ (<16 km)	0.3 ℃
	0.4 ℃ (>16 km)	
RH Range	0 - 100 %	0 - 100 %
RH Accu.	4%	2%
Horizontal WIND SPEED Accu.	0.15 m/s	0.1 m/s
		(Hor. Accu.: 2.5 m)

Table 4. Characteristics of Storm Tracker.

Characteristic	Storm Tracker
Sensors	Temperature, Humidity, Pressure, GPS location, Wind Speed
Frequency	432 MHz to 436.5 MHz
Channels	Ten simultaneous Channels
Time Resolution	1s (1Hz)
Power	1x AAA Battery
Battery Life	2 - 4 Hours
Weight	20g with 1x AAA Battery
Dimension	58.1 mm x 50.2mm x 30mm

Table 2. Characteristics of Storm Tracker.

Characteristic	Storm Tracker
Sensors	Temperature, Humidity, Pressure, GPS location, Wind Speed
Frequency	432 MHz to 436.5 MHz
Channels	Ten simultaneous Channels
Time Resolution	1s (1Hz)
Power	1x AAA Battery
Battery Life	2 - 4 Hours
Weight	20g with 1x AAA Battery
Dimension	58.1 mm x 50.2mm x 30mm

Table 3. Temperature and Humidity Error (Storm Tracker minus Vaisala RS41-SGP) Statistics for the second intercomparison experiment in July 2018 at Wu-Chi.

	Temperature Error (˚C)		Humidity Error (%)	
	W/o hat	With Hat	W/o hat	With Hat
Night Time	0.16±0.39	1.29±0.54	5.63±3.46	1.82±3.45
Day Time	2.98±1.61	2.61±1.23	-3.47±6.44	-2.43±5.3
Total	1.52±1.82	1.93±1.15	1.23±6.84	-0.23±4.92

Table 3. Temperature and Humidity Error (Storm Tracker minus Vaisala RS41-SGP) Statistics for the second intercomparison experiment in July 2018 at Wu-Chi.

	Temperature Error (˚C)		Humidity Error (%)	
	W/o hat	With Hat	W/o hat	With Hat
Night Time	0.16±0.39	1.29±0.54	5.63±3.46	1.82±3.45
Day Time	2.98±1.61	2.61±1.23	-3.47±6.44	-2.43±5.3
Total	1.52±1.82	1.93±1.15	1.23±6.84	-0.23±4.92

Table 4. Average time-lag for the second intercomparison experiment in July 2018 at Wu-Chi.

Configuration	Height				
	200~3000m	3000~4500m	4500m~end	Average	
With Hat	6.90	7.50	8.80	7.73	Seconds
Without Hat	4.70	5.60	7.80	6.03	Seconds

Table 4. Average time-lag for the second intercomparison experiment in July 2018 at Wu-Chi.

Configuration	Height				
	200~3000m	3000~4500m	4500m~end	Average	
With Hat	6.90	7.50	8.80	7.73	Seconds
Without Hat	4.70	5.60	7.80	6.03	Seconds

Table 5. All the sensor error (Storm Tracker minus Vaisala RS41-SGP) statistics for the second intercomparison experiment in July 2018 at Wu-Chi.

	W/o hat	With Hat
Temperature (°C)	1.52±1.82	1.93±1.15
Humidity(%)	1.23±6.84	-0.23±4.92
Pressure(hPa) *initial	2.76±1.29	2.59±1.5
Pressure(hPa) *with offset	0.33±1.06	0.43±1.71
Speed(m/s)	0.037±0.628	0.046±0.521
Direction(degree)	1.19±26.5	0.595±28
Height(m)	-4.5±16.7	-3.4±19.3

Table 5. All the sensor error (Storm Tracker minus Vaisala RS41-SGP) statistics for the second intercomparison experiment in July 2018 at Wu-Chi.

	W/o hat	With Hat
Temperature (˚C)	1.52±1.82	1.93±1.15
Humidity(%)	1.23±6.84	-0.23±4.92
Pressure(hPa) *initial	2.76±1.29	2.59±1.5
Pressure(hPa) *with offset	0.33±1.06	0.43±1.71
Speed(m/s)	0.037±0.628	0.046±0.521
Direction(degree)	1.19±26.5	0.595±28
Height(m)	-4.5±16.7	-3.4±19.3

Figures

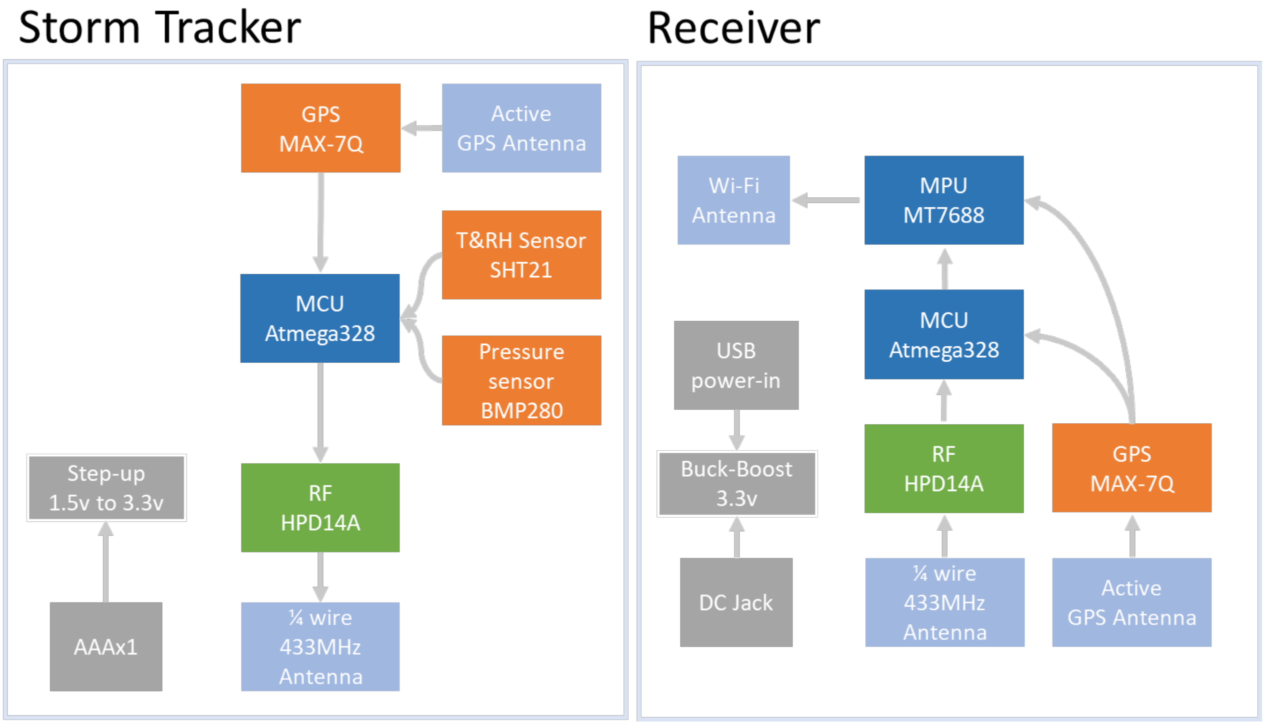

Figure 1. System block diagram for the Storm Tracker system, including Storm Tracker (left) and Receiver (right). The part number for the chipset is indicated in the box, and the arrow indicated the dataflow.

Figures

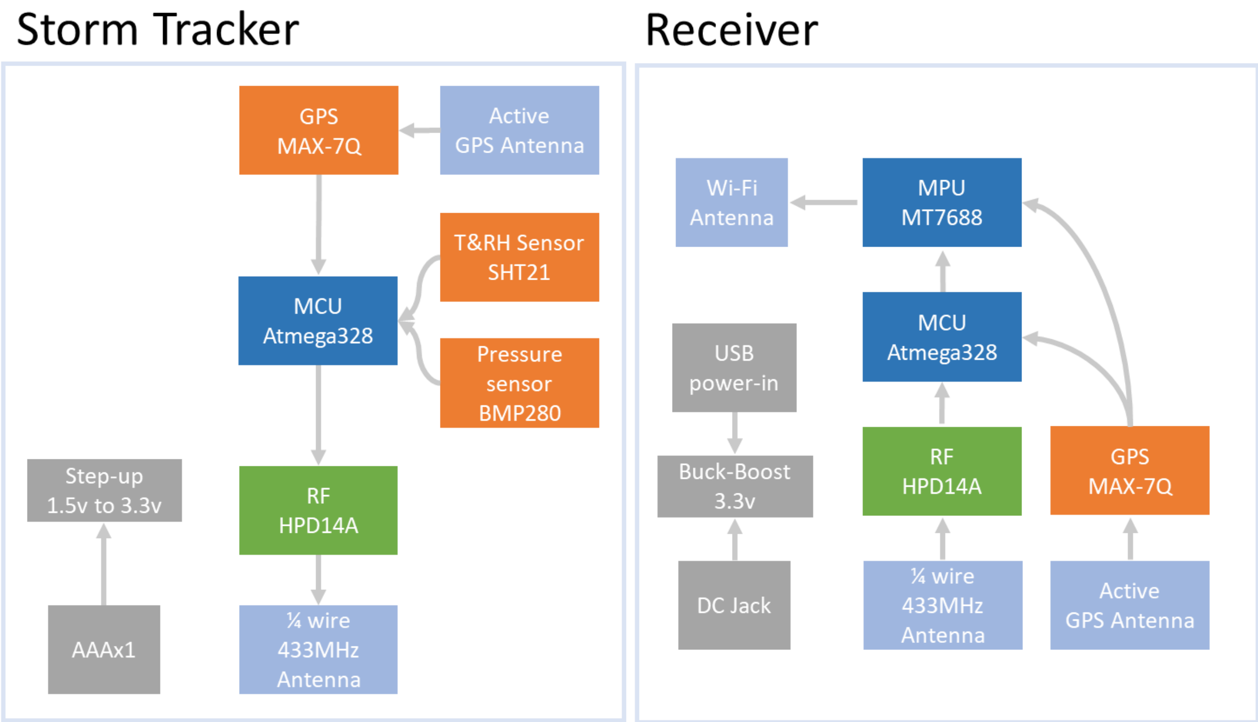

Figure 1. System block diagram for the Storm Tracker system, including Storm Tracker (left) and Receiver (right). The part number for the chipset is indicated in the box, and the arrow indicated the dataflow.

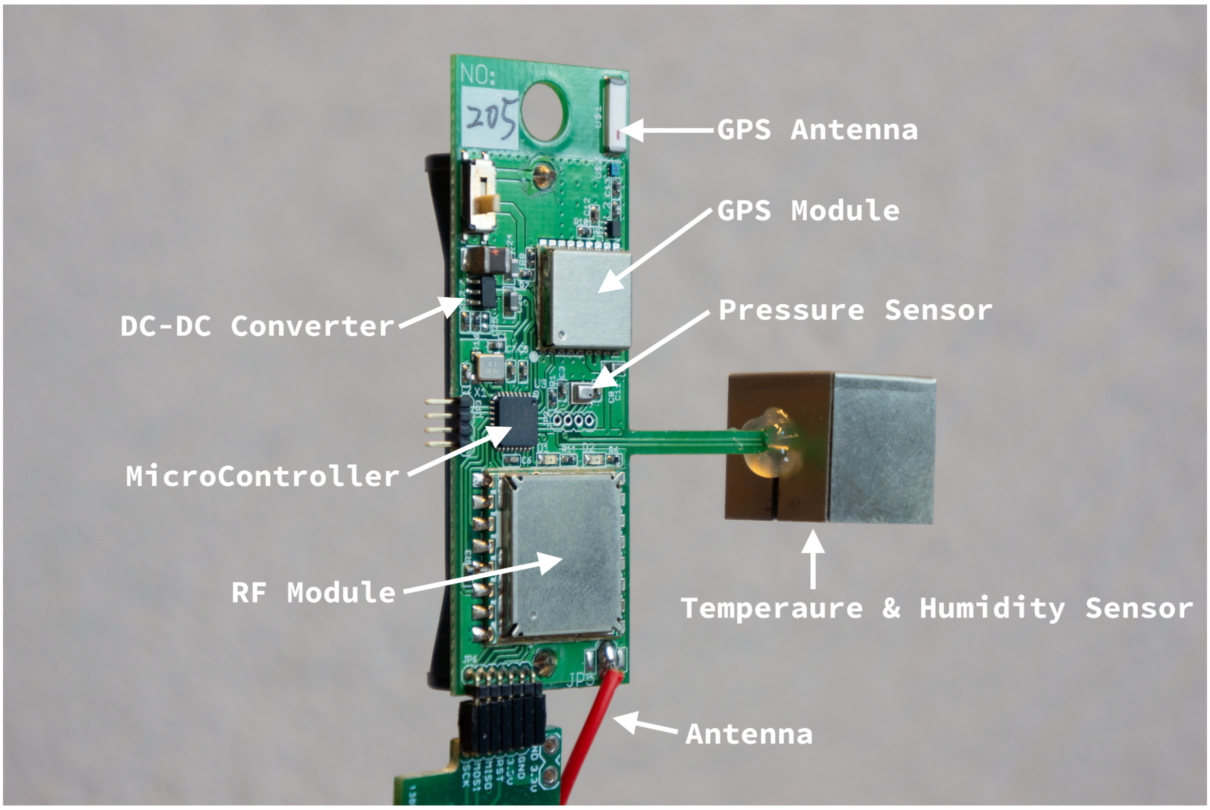

Figure 2. Photo of a PCB assembled Storm Tracker product from the PCBA. The diameter of the Storm Tracker is 58.1mm x 50.2mm (height x width, including sensor arm). The GPS antenna and GPS module are located on the top right of Storm Tracker, along with the power switching on the top left. The RF module is located on the bottom, and the red wire is the quarter-wave antenna. The extended arm hosts the temperature and humidity sensor, and the pins on the bottom are for programming and debug purposes. Lastly, in the middle are the microcontroller and pressure sensor.

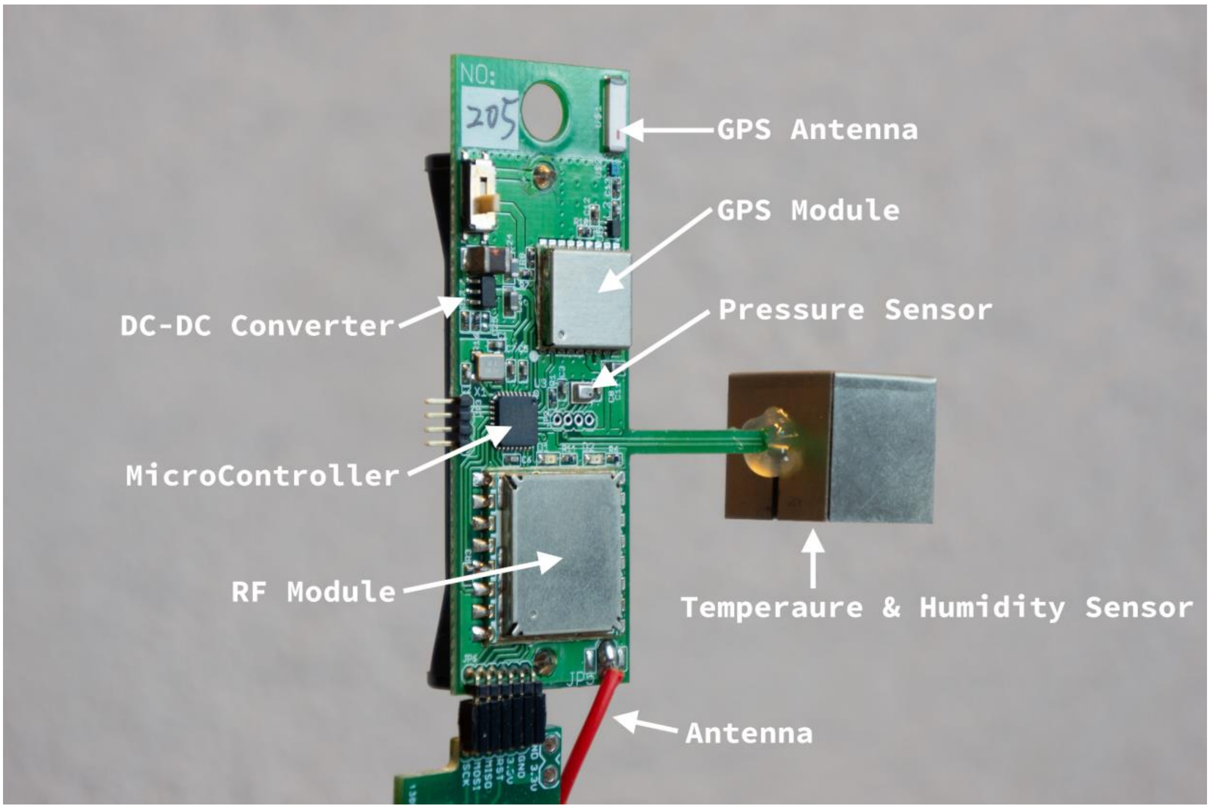

Figure 2. Photo of a PCB assembled Storm Tracker product from the PCBA. The diameter of the Storm Tracker is 58.1mm x 50.2mm (height x width, including sensor arm). The GPS antenna and GPS module are located on the top right of Storm Tracker, along with the power switch on the top left. The RF module is located on the bottom, and the red wire is the quarter-wave antenna. The extended arm hosts the temperature and humidity sensor, and the pins on the bottom are for programming and debug purposes. Lastly, in the middle are the microcontroller and pressure sensor.

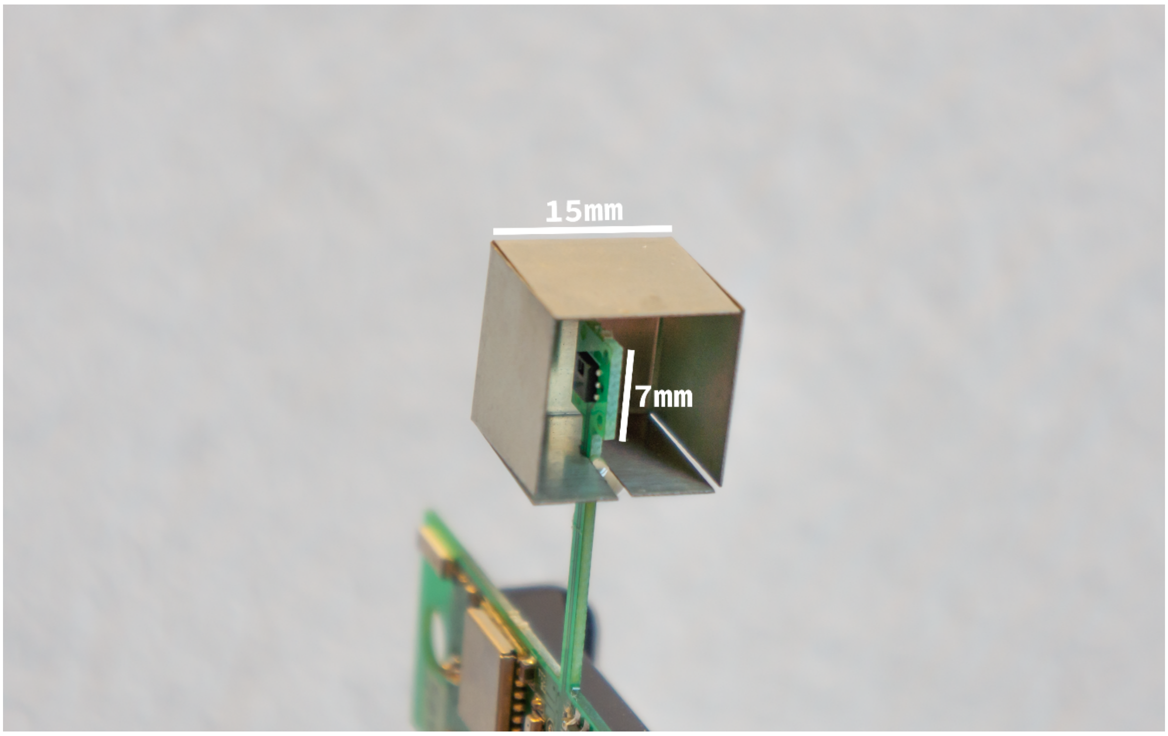

Figure 3. A closeup picture of the metal shield. The metal shield is a 15mm x 15mm x 15mm square cube, and the inner sensor PCB is a 7mm x 7mm square.

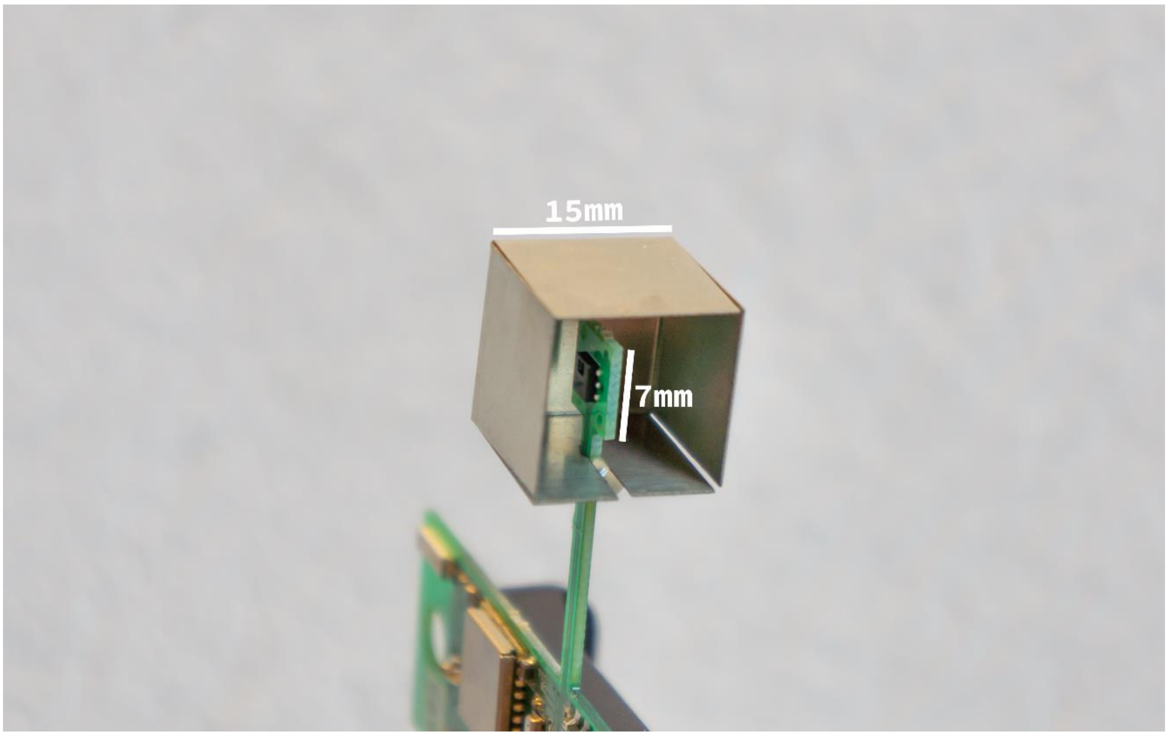

Figure 3. A closeup picture of the metal shield. The metal shield is a 15mm x 15mm x 15mm square cube, and the inner sensor PCB is a 7mm x 7mm square.

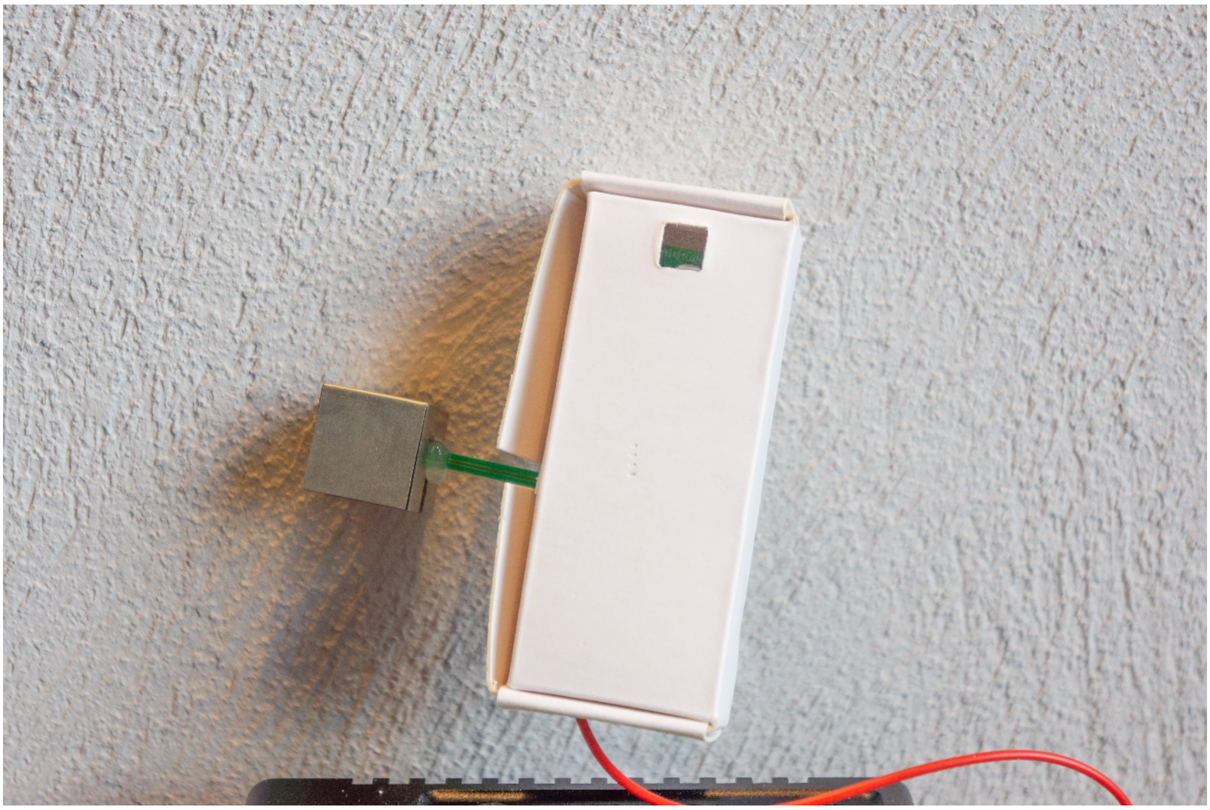

Figure 4. A Storm Tracker with the enclosure and the metal shield. The enclosure is composed of paper, and the hole on the top (bottom) is for connecting to the balloon (passing of the antenna). The metal shield is attached to the PCB board with hot glue.

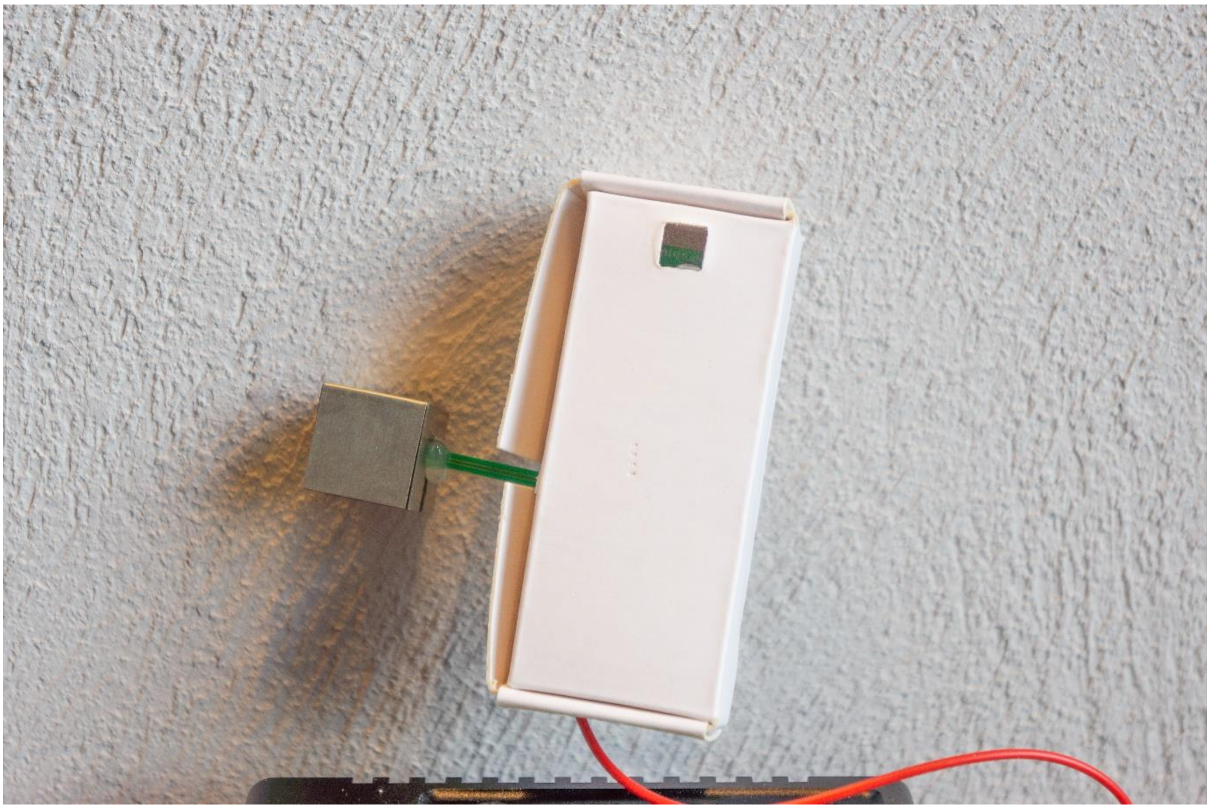

Figure 4. A Storm Tracker with the enclosure and the metal shield. The enclosure is composed of paper, and the hole on the top (bottom) is for connecting to the balloon (passing of the antenna). The metal shield is attached to the PCB board with hot glue.

Figure 5. A Storm Tracker (without enclosure) launched with a pilot rubber balloon (20g) during a field campaign.

Figure 5. A Storm Tracker (without enclosure) launched with a pilot rubber balloon (20g) during a field campaign.

Figure 6. Photo of a Storm Tracker Ground Receiver. On the right are the GPS module and RF module to receive the signal, along with the USB and DC power jack for power input and the console access. In the middle is the central processor, which handles data recording and hosts the website. On the left is the SD card for storage. On the top are the indicator LEDs, which show the current status of the receiver and the received data channels.

Figure 6. Photo of a Storm Tracker Ground Receiver. On the right are the GPS module and RF module to receive the signal, along with the USB and DC power jack for power input and the console access. In the middle is the central processor, which handles data recording and hosts the website. On the left is the SD card for storage. On the top are the indicator LEDs, which show the current status of the receiver and the received data channels.

Figure 7. A typical setup of the ground receiver in the field, with the 433Mhz antenna in the middle, and the receiver, GPS antenna and power bank at the bottom black box.

Figure 7. A typical setup of the ground receiver in the field, with the 433Mhz antenna in the middle, and the receiver, GPS antenna and power bank at the bottom black box.

Figure 8. A photo of the intercomparison launch setup. The Storm Tracker is attached to the side of a Vaisala RS41 radiosonde with double side tape.

Figure 8. A photo of the intercomparison launch setup. The Storm Tracker is attached to the side of a Vaisala RS41 radiosonde with double side tape.

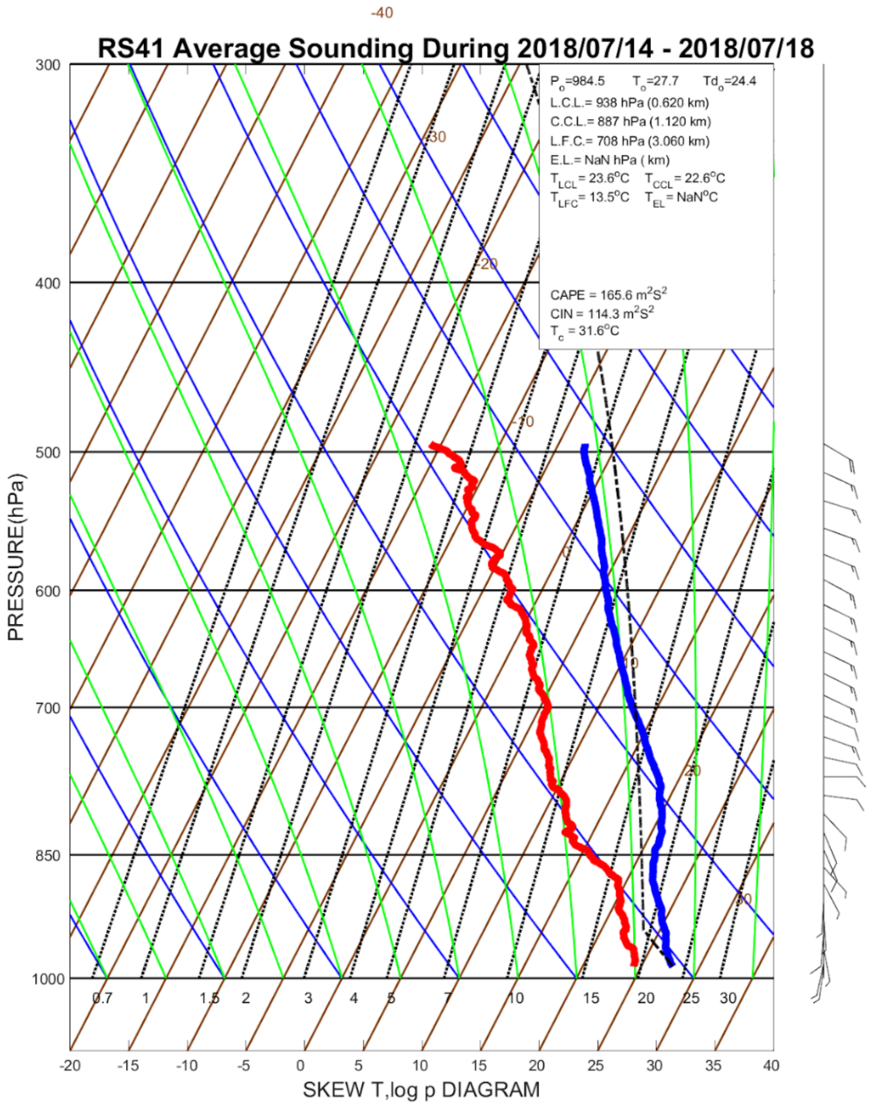

Figure 9. The skew-T-log-P diagram of the average vertical profile measured by Vaisala RS41 radiosondes during the intercomparison run in July 2018 at Wu-Chi. The thick red line indicated the dew point, and the thick blue line indicated the temperature profile.

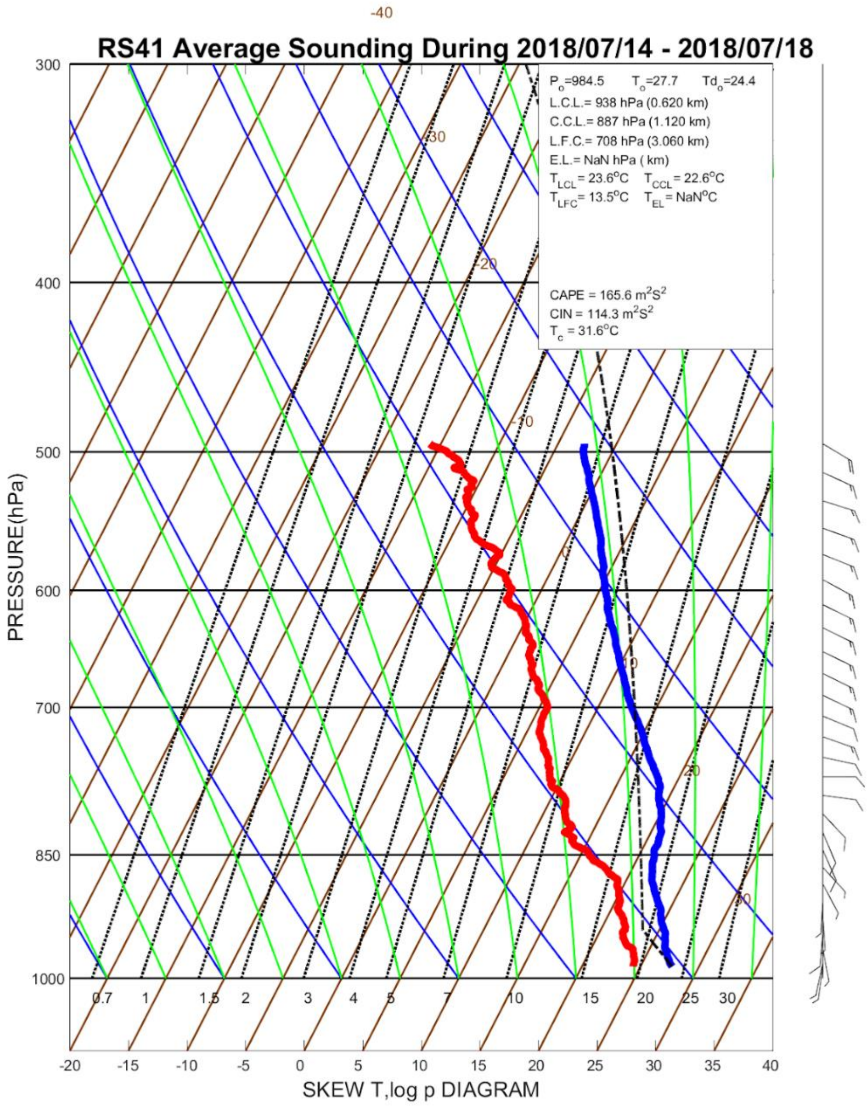

Figure 9. The skew-T-log-P diagram of the average vertical profile measured by Vaisala RS41 radiosondes during the intercomparison run in July 2018 at Wu-Chi. The thick red line indicated the dew point, and the thick blue line indicated the temperature profile.

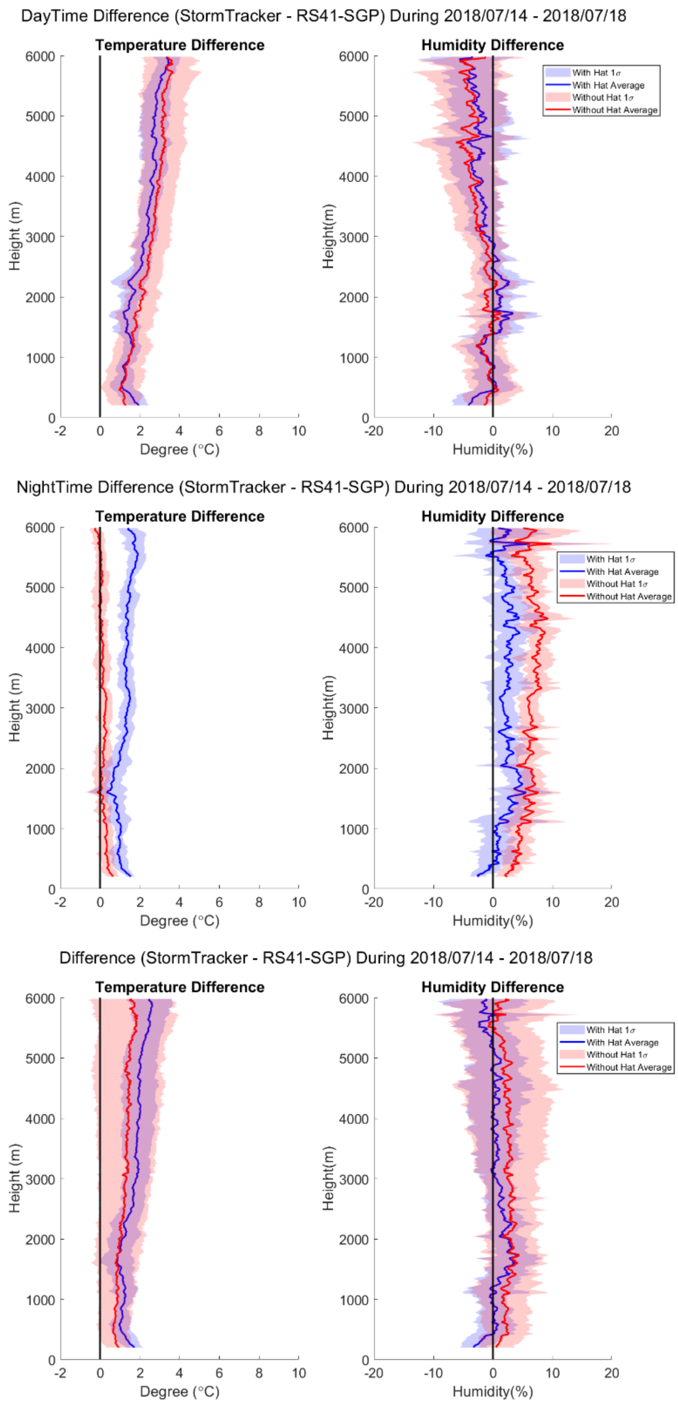

Figure 10. (a) top (b) middle (c) bottom The vertical profiles for temperature and humidity differences during both the daytime and nighttime in July 2018 at Wu-Chi experiment. The lines indicated the mean, and the one standard deviation ranges are shaded. The red color indicates daytime data, and blue color indicates nighttime data.

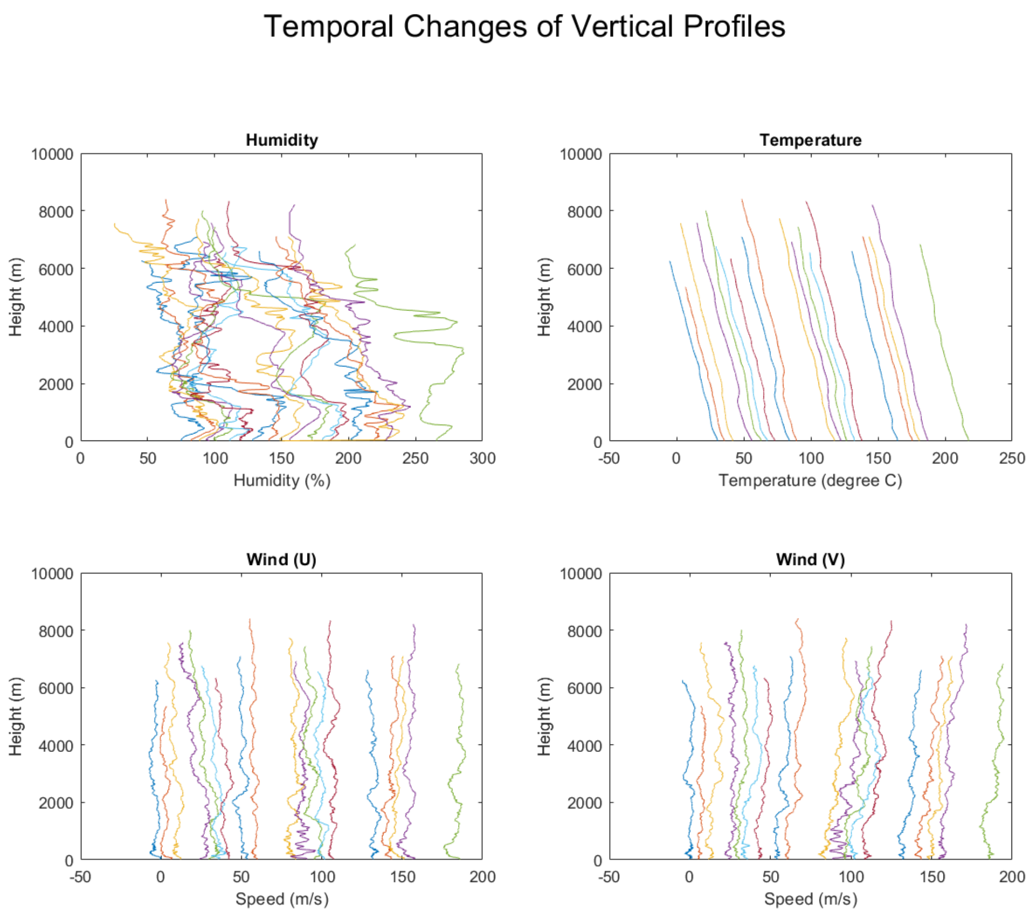

Figure 10. Temporal changes in the vertical profile during the intercomparison run in July 2018 at Wu-Chi. Each vertical profile was shifted according to the launch time. Here we added 2% per hour to humidity data, 2 °C per hour for temperature data, 2 m/s per hour for Wind data.

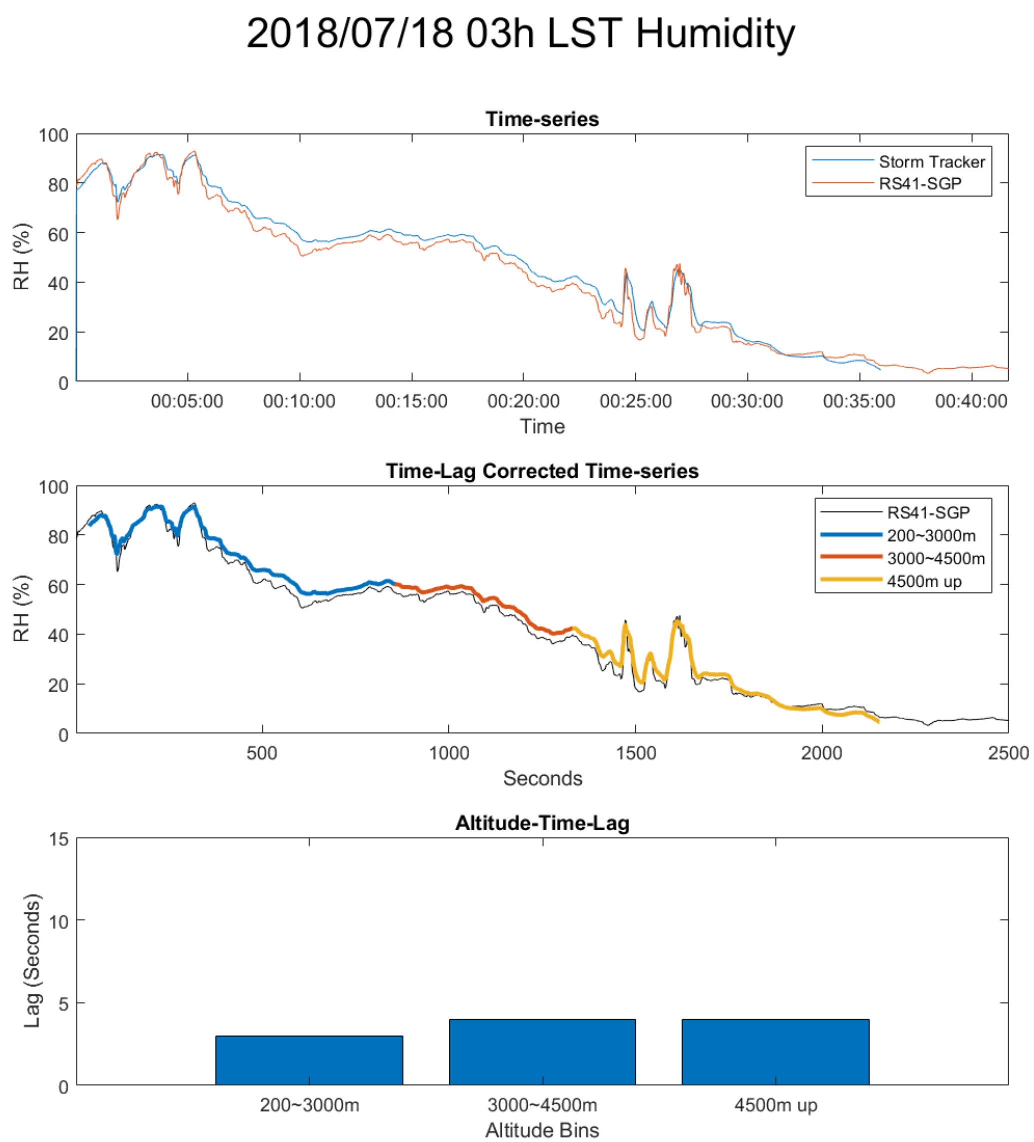

Figure 11. One of the launch data for time-lag analysis, the original time-series data, is at the top. And the time-lag corrected time-series in the middle, with three segments of the time series data for three altitude bins. And lastly, the altitude to time-lag plot at the bottom.

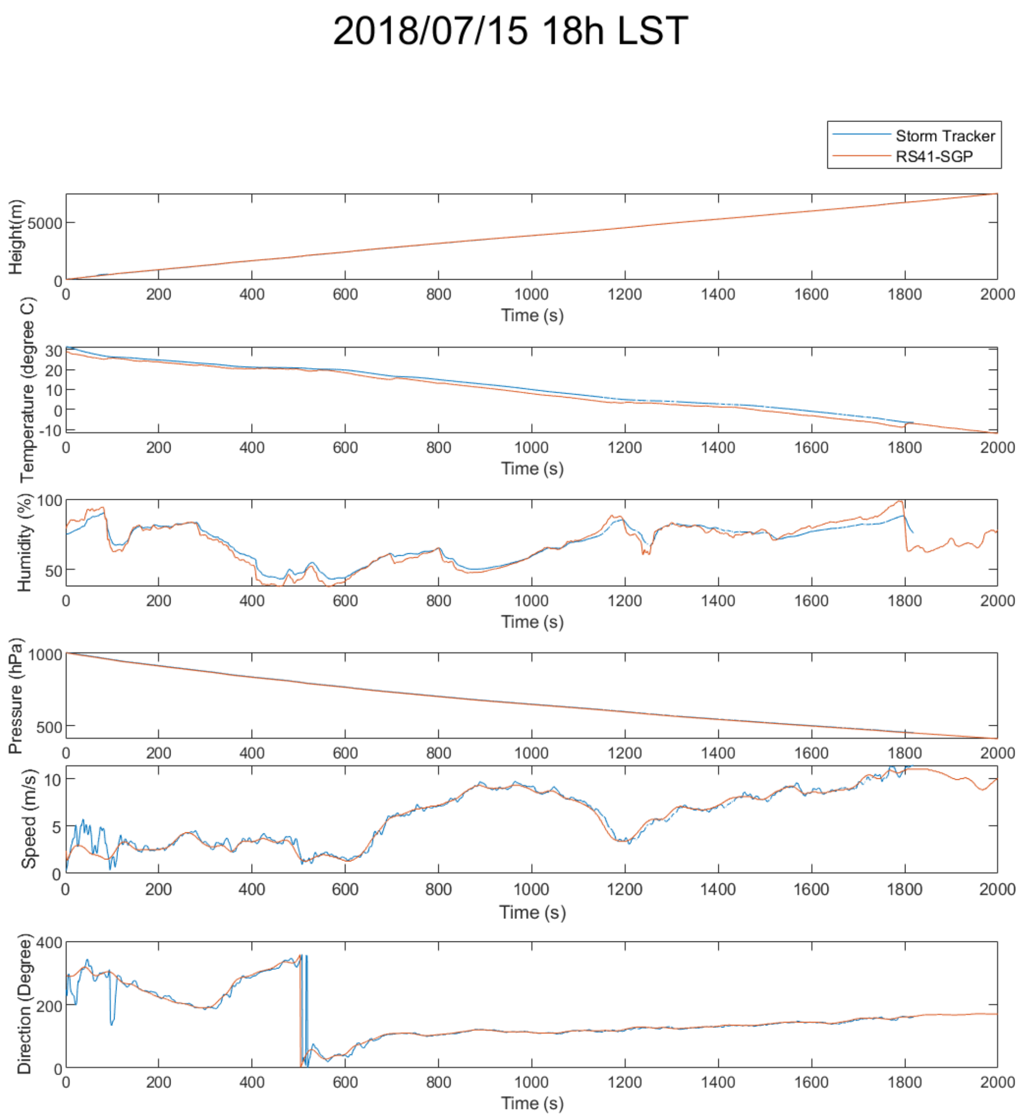

Figure 11. One of the time series comparisons during the intercomparison run in July 2018 at Wu-Chi. The blue line indicates Storm Tracker time-series data, and the orange line indicates RS41-SGP time series data.

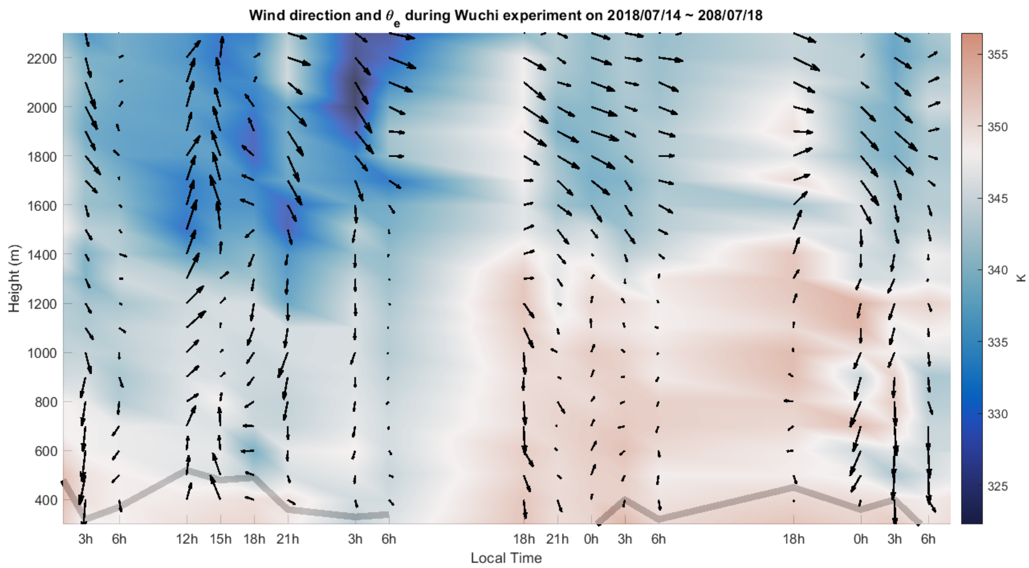

Figure 12. The time-series-height data for the experiment done during July 2018 at Wu-Chi. The shaded color represents $\boldsymbol{\theta_e}$ and the arrow direction indicates wind direction with length indicate the wind speed. Lastly, the gray line is the boundary height calculated with the algorithm developed by Liu and Liang in 2010.

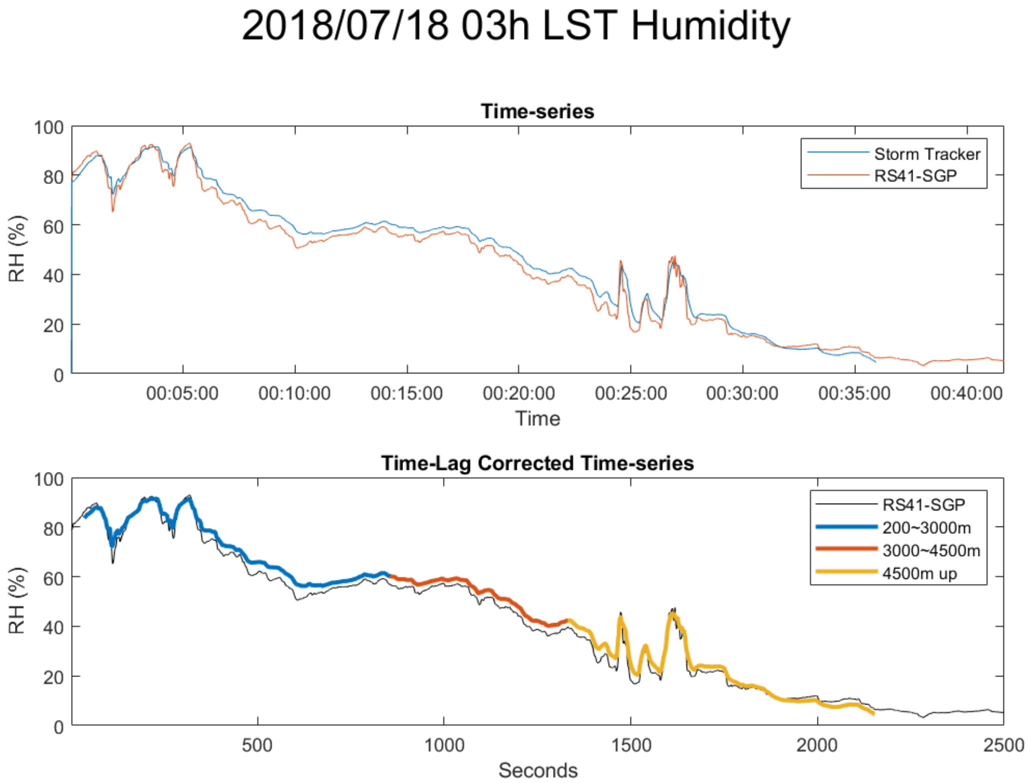

Figure 12. One of the launch data for time-lag analysis, the original time-series data, is at the top. And the time-lag corrected time-series in the middle, with three segments of the time series data for three altitude bins. And lastly, the altitude to time-lag plot at the bottom. The time lag for this case is 2s (200~3000m), 4s (3000~4500m) and 4s (4500m up).

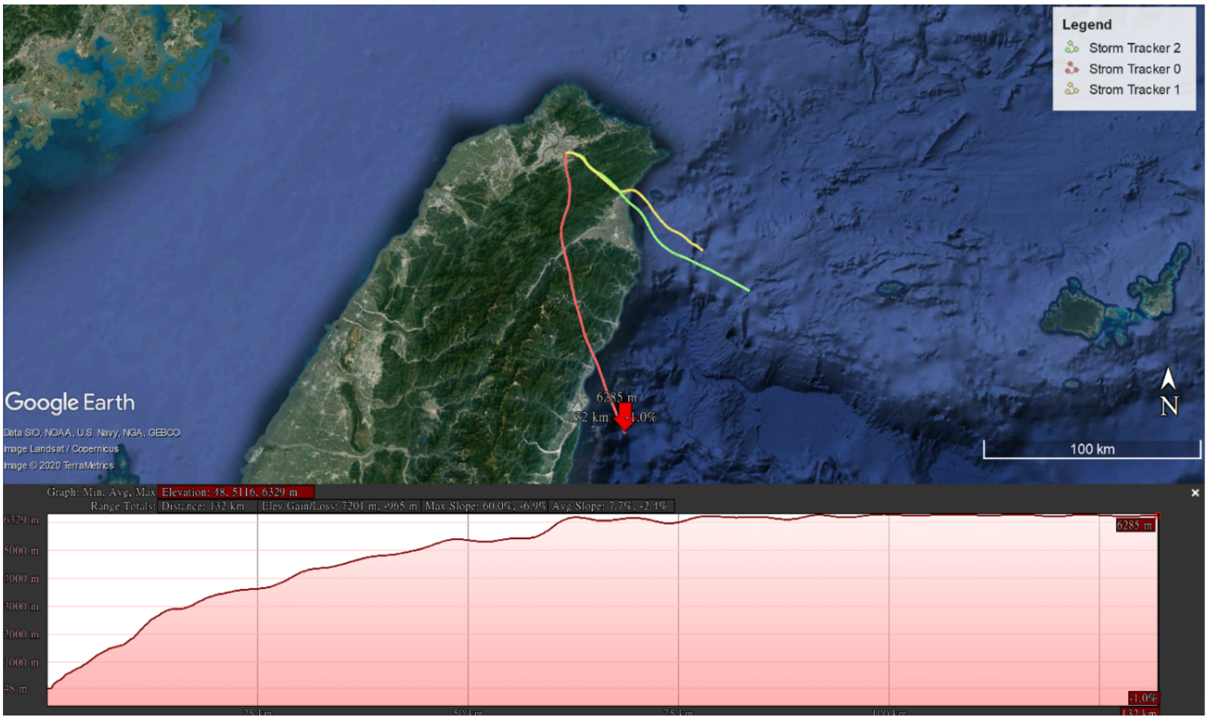

Figure 13. Three balloon tracks during Typhoon Talim (top) and the height profile of the Storm Tracker 0 (bottom). The height profile at the bottom is the time series data with time at the x-axis and height(meter) at the y-axis. The launching site is located on the campus of National Taiwan University. The maximum range of the Storm Tracker from the site is 132km, in which the Storm Tracker could maintain at about 6200m height. Credit to Google Earth Pro for providing the satellite image.

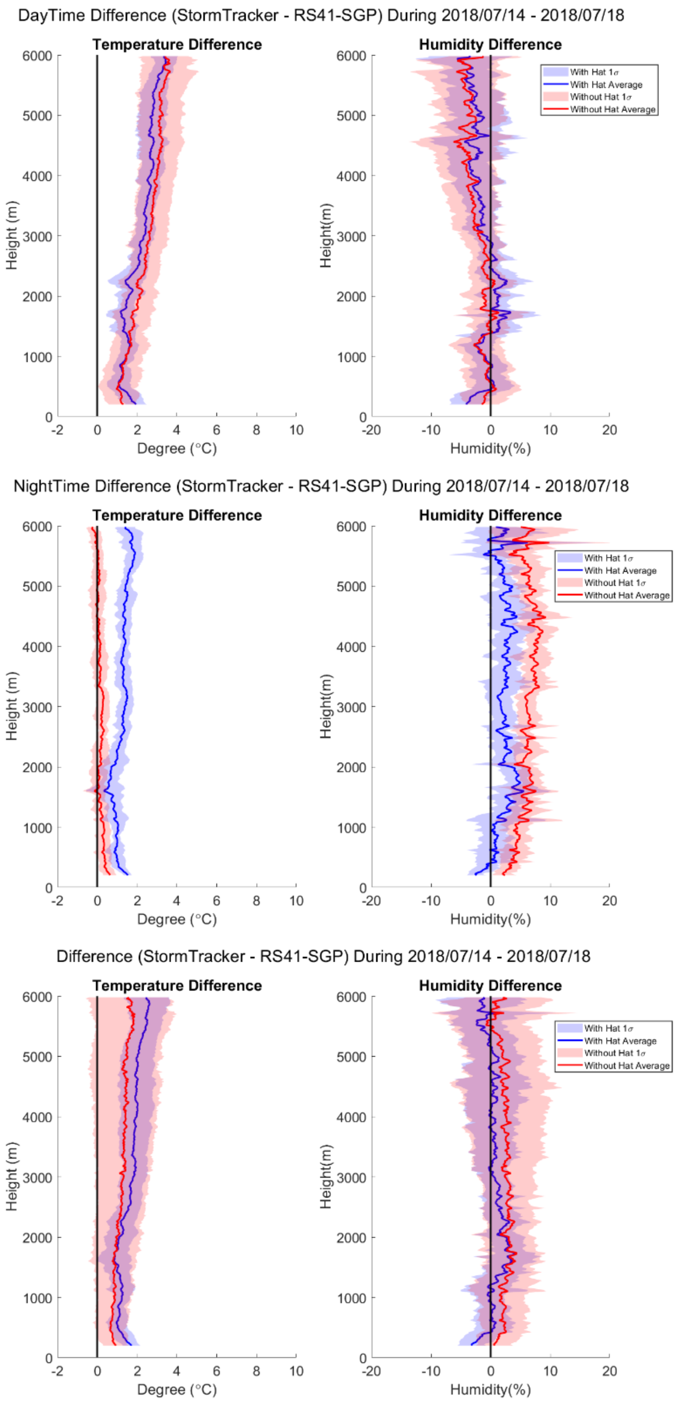

Figure 13 (a) top (b) middle (c) bottom. The vertical profiles for temperature and humidity differences during both the daytime and nighttime in July 2018 at Wu-Chi experiment. The lines indicated the mean, and the one standard deviation ranges are shaded. The red color indicates daytime data, and blue color indicates nighttime data.

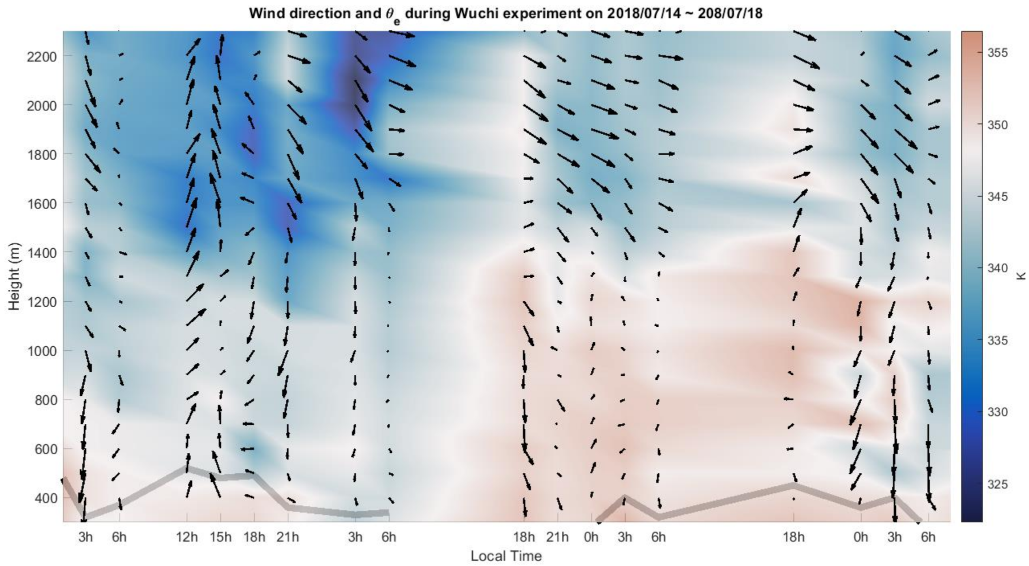

Figure 14. The time-series-height data for the experiment done during July 2018 at Wu-Chi. The shaded color represents θ_e and the arrow direction indicates wind direction with length indicate the wind speed. Lastly, the gray line is the boundary height calculated with the algorithm developed by Liu and Liang in 2010.

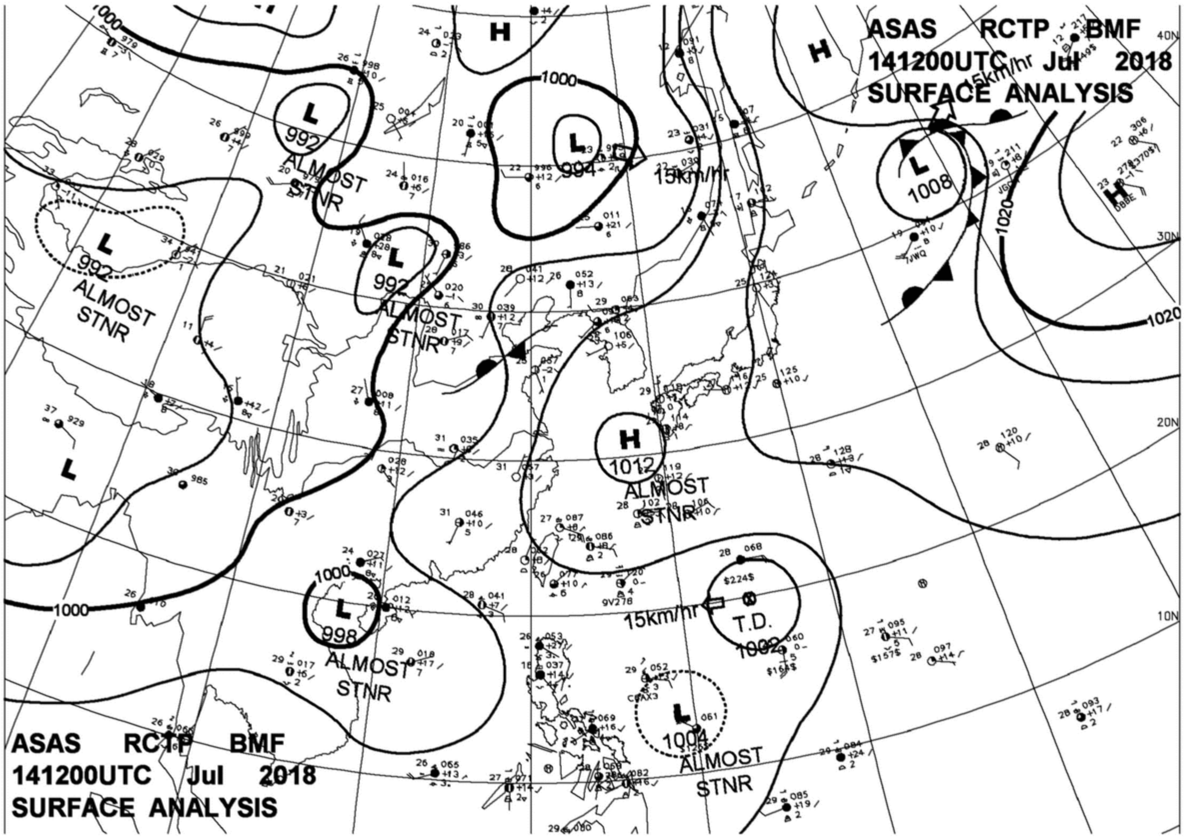

Figure 15. Surface synoptic weather chart at 12Z, July 14, 2018. Credit to Central Weather Bureau in Taiwan.

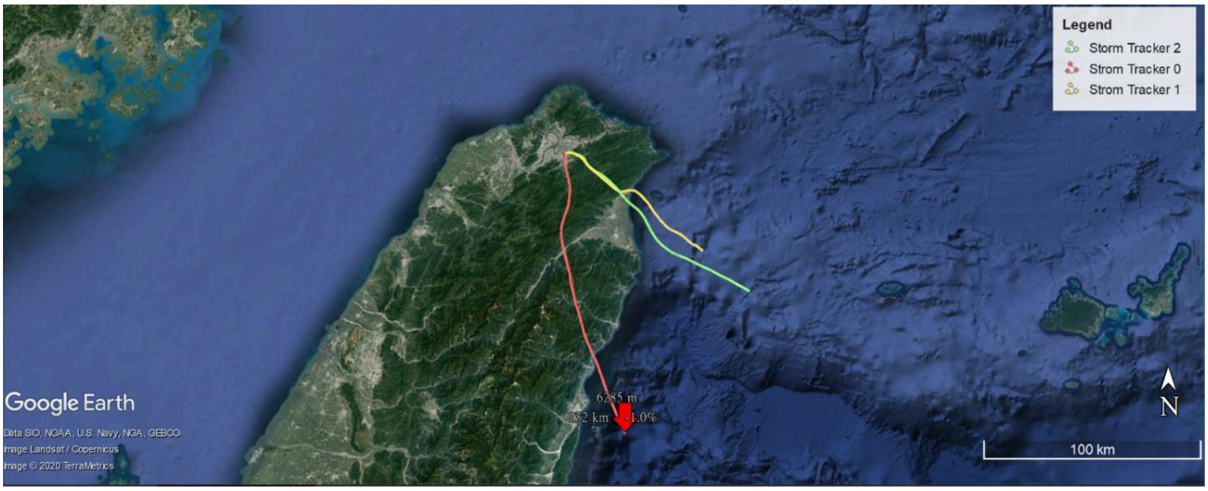

Figure 16. Three balloon tracks during Typhoon Talim (Red, yellow, and green tracks are Storm Tracker 0, 1, and 2). The launching site is located on the campus of National Taiwan University. The maximum range of the Storm Tracker from the site is 132km. Credit to Google Earth Pro for providing the satellite image.

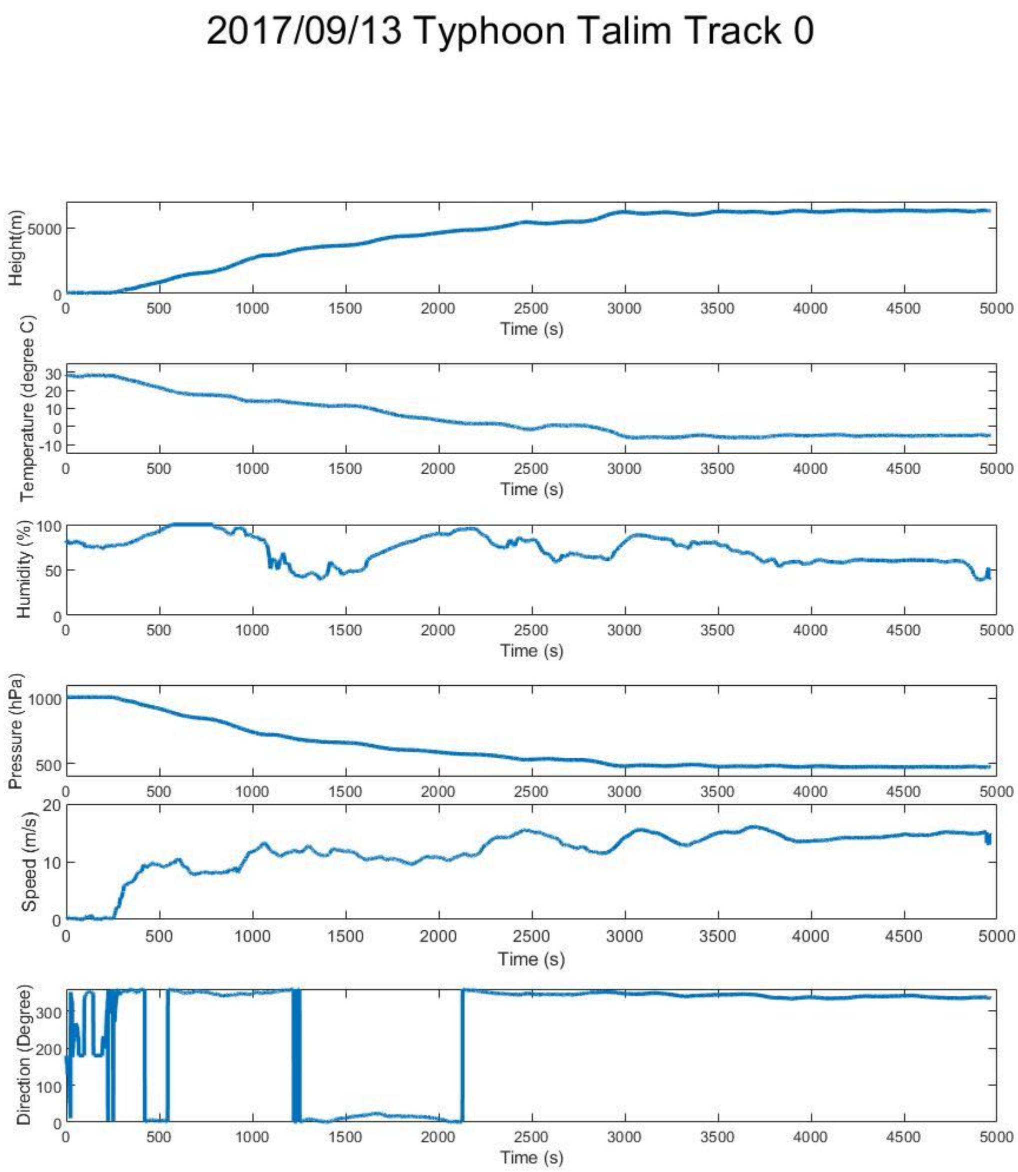

Figure 17. Storm Tracker 0 time-series data during Typhoon Talim. The altitude of Storm Tracker can maintain at around 6200 meters.